Fluidic Drag in Horizontal Directional Drilling and its Application in Specific Energy

by

Ashkan Faghih

A thesis submitted in partial fulfillment of the requirements for the degree of

Master of Science

in

Construction Engineering and Management

Department of Civil and Environmental Engineering
University of Alberta

Abstract

Horizontal Directional Drilling (HDD) is one of the most rapidly growing technologies for utility installation under surface obstacles. The rapid growth in application of HDD has not accompanied the same level of development in engineering design procedures and efficient drilling techniques. Rational engineering design and maximized drill rate are of a great value particularly in longer HDD crossings where the project budgets are in the order of millions of dollars and daily delays cost tens of thousands of dollars (Baumert and Allouche, 2002).

To improve predictions of pulling load by current design practices, exact equations for annular flow are derived in this thesis to accurately compute the fluidic drag during HDD operations. Comparisons of the exact solution with the predictions by design procedures such as PRCI and ASTM 1962 reveal that PRCI overestimates the fluidic drag while ASTM F1962 results in a better estimation.

To maximize the rate of penetration and identify underground drilling risks, the concept of Specific Energy (SE) of drilling is proposed here to be used in HDD. SE has been implemented successfully in oil and gas industry as a useful efficiency indicator of drilling operations. To calculate the real SE used by the bit to excavate the material, downhole drilling data should be measured during the process. Utilization of sophisticated downhole measuring tools is not economical in HDD. Therefore, a mechanical model is developed to calculate downhole loads and

torques using the result of the previous analysis on the fluidic drag. Finally, an example application of SE in HDD is illustrated in a case study and the SE analysis for surface and downhole conditions are presented.

Acknowledgements

I wish to express my sincere gratitude to my supervisor, Dr. Alireza Bayat, for his supports and friendly attitude during my master program at the University of Alberta.

I would like to thank Mr. Manley Osbak from the Crossing Company, for providing data and technical support to this research.

I would also like to acknowledge The Crossing Company's technical and financial contributions as well as the Natural Sciences and Engineering Research Council of Canada for providing financial support.

Special thanks to Dr. Yaolin Yi, Dr. Mahmoud Salimi, and Ms. Lauren Wozny for assisting in the editorial review of this study.

I would like to extend my deepest appreciation to my family, for their continuous support, encouragement and unconditional love.

Finally, I would like to thank my friends at the University of Alberta for their encouragement and friendship.

Table of Contents

List of Tables

List of Figures

List of Symbols and Abbreviations

$\dot{\gamma}$: Shear rate

Δp: Hydrokinetic pressure

Δp_b: Pressure drop across the bit

$\Delta p/L$: Pressure gradient

η: Energy reduction factor

θ: Inclination angle

λ: Location of maximum velocity (at $r = \lambda R$)

μ: Coefficient of friction

μ_{ea}: Effective viscosity of the drilling fluid

μ_{mud}: Mud coefficient of friction

σ: Ratio of the pipe radius to borehole radius (r_p / R)

τ: Shear stress

τ_p: Shear stress at the wall of the pipe

τ_{dp}: Viscous shear stress at the drill pipe wall due to the trip movement

τ'_{dp}: Viscous shear stress at the drill pipe wall due to the rotation

τ_{rz}: Shear stress at radius r from the centerline of the bore

ξ: Normalized radius (r/R)

A_b: Bit area

A_n: Total nozzle area

C_d: Nozzle coefficient

D_b: Bit diameter

D_{bh}: Borehole diameter

D_{dp}: Drill pipe diameter

D_p: Pipe diameter

Drag: Fluidic drag on the pipe

dp/dL: Pressure drop in the annulus

e: Specific Energy

e_h: Hydraulic component of specific energy

e_r: Rotary component of specific energy

e_t: Thrust component of specific energy

F: Thrust

F_f: Frictional force between drill pipe and borehole

F_{HK}: Hydrokinetic force or fluidic drag on the pipe

F_n: Normal force

F_v: Viscous force on drill pipe due to drilling fluid flow

K: Power Law consistency index in the annulus

L: Length of the pipe/drill pipe

MW: Mud weight

N: Rotary speed

n: Power Law flow index in the annulus

R: Borehole radius

r_p: Pipe radius

ROP: Rate of Penetration

RPM: Revolution per minute

PRCI: The Pipeline Research Council International

Q: Flow Rate

T: Torque

T_d: Fluidic drag per unit length of the pipe

W: Weight of the drill pipe element

WOB: Weight on bit

$\bar{v}$: Average mud velocity inside the annulus

v_p: Pullback speed

v_{zi}: Fluid speed within the inner region of the annulus

v_{zo}: Fluid speed within outer region of the annulus

1. Chapater 1: Introduction

1.1. Background

The rapid growing demand for new pipeline installations all over the world particularly in North America requires faster and less expensive methods to replace old and decaying utilities. Traditional cut and cover methods have been served human needs for a long time to remove, repair or install underground utilities. However, execution of these open trenching techniques is expensive and it also comes with additional costs due to the ground surface repairs including pavements, sidewalks, and curbs, and social costs arising from traffic disruptions (Ariaratnam et al., 1999).

To aim at the needs for replacing old pipelines and installing new utilities (including power, water, sewer, telecommunication, oil and gas distribution lines), alternatives to open trenching have been developed to allow less social and environmental impacts during the installation. These techniques are known as Trenchless Technologies (TT) because no digging is the key feature in them. TT methods have become advanced based on their wide range of applications such as underground utility construction, replacement, rehabilitation, renovation, repair, inspection, and leak detection (Najafi, 2010). Availability of various equipment, methods, and materials has made TT a feasible option (Allouche et al., 2000).

Among TT techniques, Horizontal Directional Drilling (HDD) is one of the most rapidly growing technologies due to its environmentally friendly procedure and wide range of applicability. HDD is a directionally controlled drilling used to drill long boreholes to install utilities and pipelines under surface obstacles (Osbak, 2011). In deep installations or crossings beneath rivers, lakes and highways, HDD is more economical and viable than any other trenchless methods (Atalah, 2009).

In 1990's, HDD industry was extending mostly due to rapid growth of telecom and high demands for fiber-optic installation in the United States. During the recent years, pipeline installation has become the major area of HDD market (Trenchless Technology, 2011). With continuous growing demand for energy, the need for fossil energy as the major portion of the resources is increasing. The demand for oil and gas around the globe is anticipated to increase 5.3% annually, reaching 51.8 million metric tons in 2017 (Deneen, 2013). Development of pipeline infrastructure is an inevitable response to the increasing energy productions and HDD contributes significantly to this new development. However, engineering guidelines and standards for design and monitoring of HDD operations have not developed as fast as the rapid growth in HHD acceptance and application, and design procedures have been limited particularly regarding the prediction of the pulling force during pipe installation (Baumert and Allouche, 2002). This pulling force, called pullback load, is crucial for design engineers during planning stages of HDD operations to select the appropriate product pipe and drill rig size. The product pipe should have adequate strength to avoid damages during installation while the drilling rig should

be capable of providing the required load to pull the pipe. A realistic pullback load prediction is of a great importance particularly in longer HDD crossings where the installation loads are in thousands of kilonewtons, the project budget is in millions of dollars and tens of thousands of dollars are associated with daily delays in the operation (Baumert and Allouche, 2002).

Besides the need for a rational design standard, utility companies are looking for efficient and cost effective procedures in HDD. Risk and productivity analyses of HDD operations have become paramount in recent years to investigate the impacts of different conditions and parameters. Several studies have been conducted to assess the significance of different factors affecting the HDD productivity and estimate the cost and duration of the projects (Ali et al., 2007; Mahmoud, 2009; Sarireh, 2011; Zayed et al., 2007). In all of the cited productivity studies, the drilling operation was selected as a significant portion of HDD projects in terms of the influence on HDD production rate. However, there has not been any study to address how to improve the efficiency of drilling in HDD. Techniques and technologies to practice efficient drilling in HDD are valuable particularly if they can be easily implemented without considerable costs.

Originating from oil field in 1970's, HDD technology has many similarities to oil well drilling. Oil and gas production companies are continuously seeking to reduce the time of the drilling operations to enhance cost effectiveness and earlier production of reservoirs. Several methods have been developed to optimize the drilling process ranging from sophisticated downhole measuring tools and

advanced software to different concepts and risk analysis (Provost et al., 1987; Pessier et al., 1992).

One of the common techniques to reduce the time and the risk of the drilling projects that can also benefit HDD technology is to optimize the rate of penetration (ROP) in drilling by considering the amount of specific energy (SE) required to drill the formation. The concept of SE has been used successfully in oil and gas drilling as a useful efficiency indicator. Energy surveillance helps in better understanding of the drilling mechanics and the identification of downhole problems (Bevilacqua et al., 2013). The SE is defined as the amount of energy required to excavate and remove a unit volume of material. SE relates the drilling inputs including thrust, torque, rotary speed, and hydraulic parameters to the output excavation area.

1.2. Research Impetus

In HDD pipeline installation, pullback force is a function of several factors, including the net buoyancy weight of the pipe in the borehole, the frictional forces, and the fluidic (viscous) drag (Baumert and Allouche, 2002). There has been a limited number of models proposed to predict the pullback load, each approaching the fluidic drag component differently (Driscopipe, 1993; Drillpath, 1996; Huey et al., 1996; ASTM, 1999; Polak et al., 2002). Poor agreements of the predictions by these methods with the field measurements necessitate the development of comprehensive models that better reflect the reality of pipe installation by HDD

(Duyvestyn, 2009; Baumert and Allouche, 2002). Discordant predictions for viscous drag by current design procedures have revealed the significance of having a reliable calculation method. Therefore, a new approach for calculating fluidic drag is proposed in this study based on the mechanics of drilling fluid. Furthermore, improving the efficiency of the drilling process is an important and essential step to increase the productivity and reduce the time and cost of HDD operations. Hence, SE has been selected as a useful tool in this thesis to improve the drilling efficiency in HDD crossings.

The heart of every HDD operation is the drilling rig which is set on the surface and provides the forward thrust and rotary torque to the drill bit. Drill pipes which are extended from the rig down to the bottom of the borehole transfer the force and torque to the drill bit. SE can be calculated using drilling data recorded by the rig's sensors on the surface. However, due to the friction experienced by the drill pipes in the borehole, not all the surface torque and force are available to the bit. Therefore, energy loss is inevitable during deviated and horizontal drilling. This energy loss becomes considerable when a long HDD crossing is constructed. Consequently, surveillance of surface SE may result in the assumption of higher energy consumption than what is really expended by the bit and may mislead the operator to an inefficient drilling condition. Figure 1.1 shows a schematic of difference between surface and downhole measurements.

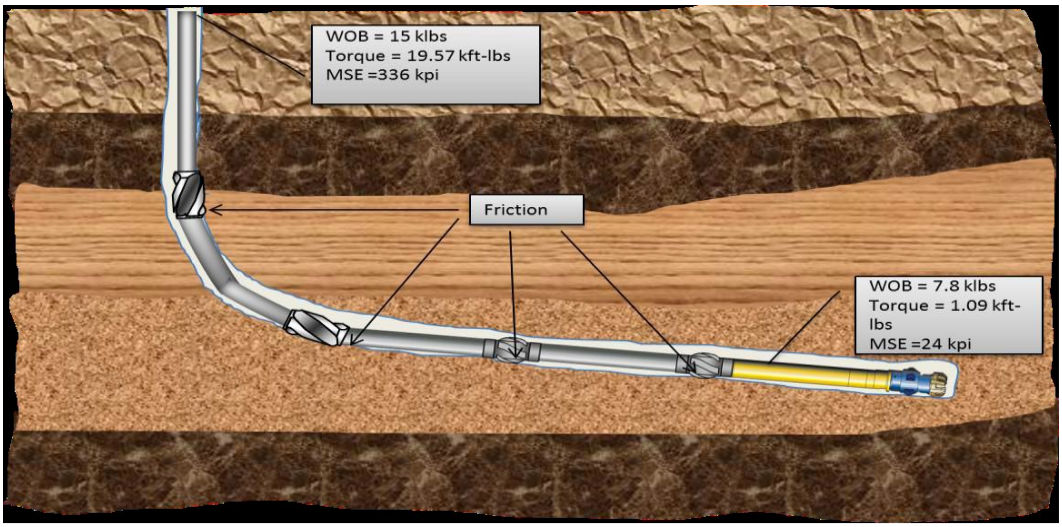

Figure 1.1. A schematic of difference between surface and downhole in a wellbore (Origho, 2012)

Calculation of SE expended by the drill bit requires the measurement of the downhole drilling parameters. With the aid of sophisticated data acquisition tools, it is now possible to record downhole data in drilling operations (Bevilacqua et al., 2013). However, these downhole measurement tools are expensive and it is not economical to use them in every drilling operation (Origho, 2012). Using the result of the fluidic drag analysis, this thesis presents a mechanical model to estimate the downhole force and torque from the surface measurement and provides the HDD operators with a tool for real-time analysis of SE.

1.3. Research Objectives

This study proposes the utilization of SE to improve the efficiency of pilot hole drilling as the first and major portion of HDD projects. To accomplish this task, a model is required to compute downhole SE particularly for longer HDD crossings. Drill pipe interaction with the borehole and the drilling fluid is the source of

difference between surface and downhole measurements. Accordingly, it is necessary to identify and analyze loads resisting the drill pipe motion in the borehole. Drill pipes are subjected to different loads during the operation. These loads can be divided as frictional force between drill pipe and borehole, gravity load due to the weight of the drill pipe, and viscous force between drill pipe and drilling fluid. For the case of calculation of the viscous force, one option is to use current HDD design procedures such as ASTM F1962 (ASTM, 1999) and the Pipeline Research Council International (PRCI) method (Huey et al., 1996; Hair et al., 2008). These methods have presented equations to estimate the viscous drag during the product pipe installation which is similar to calculate the drag acting on the drill pipe. However, inconsistent results and conflicts by their predictions became the incentive for this research to derive the exact analytical equations to estimate the viscous force acting on the drill pipe and similarly, on the product pipe during installation. Therefore, the main objectives of this study are summarized as follows:

- To derive an exact analytical solution to calculate viscous force and compare the result with the predictions by ASTM F1962 and PRCI.
- To develop a mathematical model to predict downhole force and torque by the analysis of all the loads and torques acting on the drill pipe in the borehole;
- To demonstrate the utilization of the concept of SE in HDD and calculation of surface and downhole SE in order to identify drilling problems and maximize ROP.

1.4. Methodology

This thesis is focused on viscous drag estimation and implementation of SE in HDD and it is organized into three sections. In the first section, after reviewing the important features of HDD operations, current design models to predict the fluidic drag are discussed and a comprehensive literature review was conducted to select an appropriate model to describe SE in HDD. In the second section of this study, fluid mechanics of the drilling mud in the borehole was discussed to analyze the annular flow during HDD. A case study of a pullback operation was used to compare the results gained by the proposed equations and ASTM 1962 and PRCI methods. A parametric sensitivity analysis was also conducted to investigate the influence of HDD design parameters on the fluidic drag.

The third section presents a model to predict the downhole thrust and torque from the measurements by the surface sensors in an attempt to estimate downhole SE without the implementation of expensive downhole measuring instruments. In the next step, SE was calculated in accordance with surface measurements and downhole predictions for an example case study and the importance of different components of SE was discussed.

1.5. Thesis Structure

This thesis is organized as the following:

Chapter 1 – Introduction: In this chapter, a background on HDD and importance of fluidic drag estimation and improving the efficiency of drilling operation were

presented. The thesis objectives, and the methodology and the thesis structure were discussed.

Chapter 2 – Literature Review: In this chapter, HDD technology and its different classification were described. The HDD process and the need for capturing drilling data were also discussed. Then, a brief review of the current design models to calculate fluidic drag was presented and the concept of specific energy was introduced.

Chapter 3 – Fluidic Drag Estimation in Horizontal Directional Drilling Based on Annular Flow Equations: In this chapter, a new method to calculate the fluidic drag based on the annular flow equations was presented and the result was compared to the predictions by current design practices, such as PRCI and ASTM F1962. The impacts of design factors on the fluidic drag were also investigated.

Chapter 4 – Efficient Drilling in HDD by Implementing the Concept of Specific Energy: In this chapter, a mechanical model was developed to calculate downhole loads and torques, and downhole SE as the real amount of energy expended by the bit. An example application of SE in HDD was illustrated in a case study and the calculation of surface and downhole conditions were presented.

Chapter 5 – Conclusions: In this chapter, the research approaches were summarized and the results and findings of this thesis were highlighted. Future research areas were also proposed to further develop the potentials of this research for the trenchless industry.

2. Chapter 2: Literature Review

2.1. Horizontal Directional Drilling

2.1.1. Introduction

HDD was first originated from oil industry in 1970's to install utilities under obstacles such as rivers, lakes, roads, railways, and airport runways. One of the first HDD project took place in 1971 for installation of a 10 cm (4 in) diameter steel pipe in 187 m (615 ft) length of crossing under Pajaro River near Watsonville, California (Najafi, 2005). By advancement of steering and navigation tools and integrating modern technologies from oil field, HDD received more attentions from utility companies as a feasible and cost effective alternative for open cut methods. In a short period of 15 years, HDD developed from a few number of contractors to a multibillion-dollar industry (Allouche et al., 2003). HDD utilization has been growing faster than other Trenchless Technologies (TT). In a survey conducted to rank TT methods and their applicability, HDD was selected by 87 Canadian municipalities as the greatest potential for future growth and development (Ariaratnam et al, 1999). HDD has progressed from a simple utility boring technology to a sophisticated method capable of installing over 127 cm (50 in) pipe diameter (Najafi, 2014).

HDD can be employed in a wide range of applications from the installation of oil and gas distribution network, water mains, gravity sewers, telecommunications and electrical conduits, to geotechnical investigation and environmental application

such as remediation of underground contaminated areas (Allouche et al., 2000). Superiority of HDD over other TT methods can be summarized as:

- No need for constructing a vertical shaft as the operation starts from the surface;
- Short preparation and setup time;
- Versatility in design of borehole alignment and elevation to avoid hitting other underground utilities and obstacles; and
- The longer installation length than any other non-man entry trenchless technique (Allouche et al., 2000).

2.1.2. HDD Classifications

Drill rig is the engine of HDD operations and it is used to drill the pilot hole, back ream the borehole, and pull the product pipe back to the hole. Based on the rig size, HDD industry is categorized in three main areas: maxi-HDD for large diameter, midi-HDD for medium diameter and mini-HDD for small diameter application (Najafi, 2014).

Mini-HDD rigs are used to install pipes up to 30 cm (12 in) in diameter for lengths up to 180 m (600 ft). They are mounted on a single trailer or truck as a single self-contained unit, with engine, hydraulic power, and pump. They are designed for drilling in congested urban areas to install conduits and small diameter pipes. They are mostly used to bore in soft semiconsolidated soil without any gravel and cobble (Willoughby, 2005).

Midi rigs are used to install larger diameter pipes and longer crossing length up to 305 m (1000 ft) comparing to mini-HDD. Their setup space is still sufficiently compact to be used in urban area for installation of municipal utilities while they can be also employed for large diameter river crossings. They can drill in unconsolidated or consolidated soil (Willoughby, 2005).

Maxi rigs require large setup areas and they are primarily used in pipeline installation. They are designed to bore holes several thousand feet in length and install pipe up to 150 cm (60 in). Based on their application, other supplementary units should be installed including, drill pipe trailer, drilling fluid circulation system, water tanks, pump and hose (Willoughby, 2005). The larger drilling rigs are cable of giving over 4450 kN (1,000,000 lb) of thrust and drill long distances and can consist of more than 20 trailer loads (Osbak, 2011). Table 2.1 compares the main features of different categories of HDD.

Table 2.1. Comparison of different HDD methods (Najafi, 2005)

Type	Diameter (in)	Depth (ft)	Drive length (ft)	Torque (ft-lb)	Thrust/ pullback (lb)	Machine weight (ton)	Typical application
Maxi	24 to 60	≤200	≤6000	≤80,000	≤100,000	≤30	River, highway crossings
Midi	12 to 24	≤75	≤1000	900 to 7000	20,000 to 100,000	≤18	Under rivers and roadways
Mini	2 to 12	≤15	≤600	≤950	≤20,000	≤9	Telecom and power cables, and gas lines

Figures 2.1 and 2.2 show maxi and midi HDD rigs with thrust of 2780 kN (625,000 lb) and 356 kN (80,000 lb), respectively.

Figure 2.1. A maxi-HDD with 2780 kN (625,000 lb) thrust (Osbak, 2011)

Figure 2.2. A midi-HDD with 356 kN (80,000 lb) thrust (Osbak, 2011)

2.1.3. HDD Process

An HDD installation consists of three stages:

- Pilot hole drilling;
- Reaming; and
- Pullback.

The process is summarized here:

2.1.3.1. Pilot Hole Drilling

After setting up the drill rig and other supporting equipment on the entry location of the designed drilling path, a small diameter drill pipe with a cutting face at the head penetrates the ground. The entry angle between the drilled bore and the surface is between 8 and 16 degrees. When reaching the desired depth, drill pipe is bent to follow the drill path and it gradually comes up to the surface again from the exit point with an angle of 8 to 12 degrees (Najafi, 2005). Figure 2.3 shows a schematic of the pilot hole drilling stage. Design of bore path usually includes an entry straight section, followed by a bent to reach a prescribed depth and then, it becomes horizontal. Another bent is planned to make the direction of the drill pipe upward and an exit line brings it to the surface. To trace the location of the cutterhead, a probe is situated close to the bit which sends information regarding horizontal and vertical coordinates of the drilling tool to the operator. The operator checks the location of the cutting tool periodically to make sure that it follows the predetermined path.

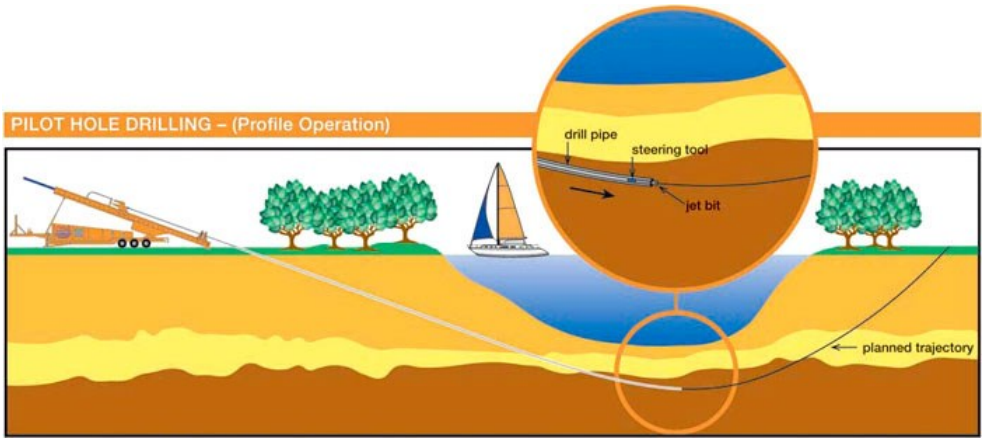

Figure 2.3. Pilot hole drilling stage of HDD (Courtesy of Trackson Horizontal Drilling Pty Ltd.)

Pilot hole is bored by the forward thrust and rotation of the cutterhead provided by the drill rig and the impact force of the drilling fluid inserted to the face of the borehole through the nozzles on the drilling tool. The drilling tool used in HDD can be range from a slim cutting head with a slanted face for mini-HDD applications to a diamond-mounted roller bits used with a mud motor for maxi projects (Najafi, 2005). Figure 2.4 shows a tri-cone roller bit used to cut compacted soil to hard rocks. During the process, a drilling fluid is continuously injected through the drill pipe down to the drill bit and exits from the nozzles. Drilling fluid functions to stabilize the borehole, cool and lubricate the drilling equipment, transfer cuttings to the surface, increase the rate of penetration, and fill the annulus after the product pipe is installed (Ariaratnam et al., 2007).

Figure 2.4. A tri-cone roller bit (Courtesy of Ditch Wich)

2.1.3.2. Reaming

Figure 2.5 shows the reaming process in HDD. Once the pilot hole is drilled successfully, the hole needs to be expanded to usually 50 percent larger than the product pipe diameter. This step may be skipped for small conduit and utility installation when the pilot hole is large enough. Downhole drilling tools are replaced with a reamer at the end of the drill pipes and the reamer is pulled to enlarge the bore. Drill pipes are generally pulled from the exit side to the rig side. The reamer enlarges the borehole while the injected drilling mud stabilizes the hole and transfers the cuttings to the surface. Based on the soil condition and final product pipe size, a certain number of reaming runs may be performed to enlarge the hole to the desired diameter.

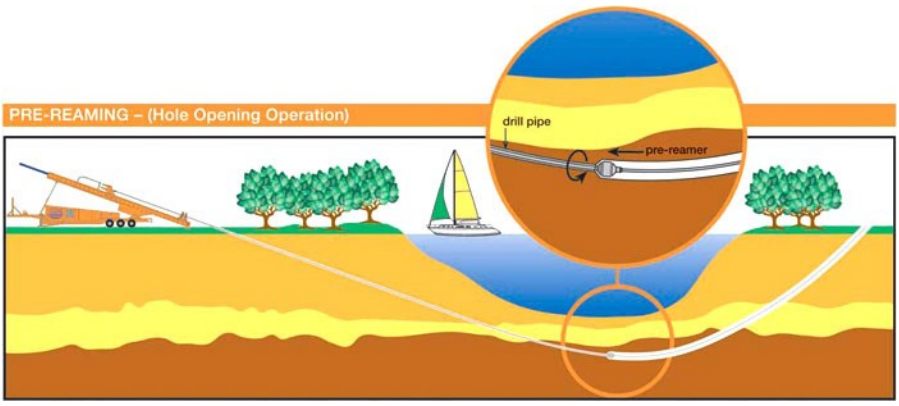

Figure 2.5. Reaming process in HDD (Courtesy of Trackson Horizontal Drilling Pty Ltd.)

2.1.3.3. Pullback

In the last step, it is the time to install the prefabricated pipeline rested on the opposite side of the rig. The drill pipe is attached to the pipe via a pull head and a swivel. A reamer is usually located between the pull head and the drill pipe to clear the path for the pipeline from any remaining cuttings and allow the drilling fluid to be pumped into the hole (Figure 2.6). The swivel prevents any rotation transferred to the pipeline in order to have a smooth pull into the hole. Figure 2.7 shows the components of the pullback operation.

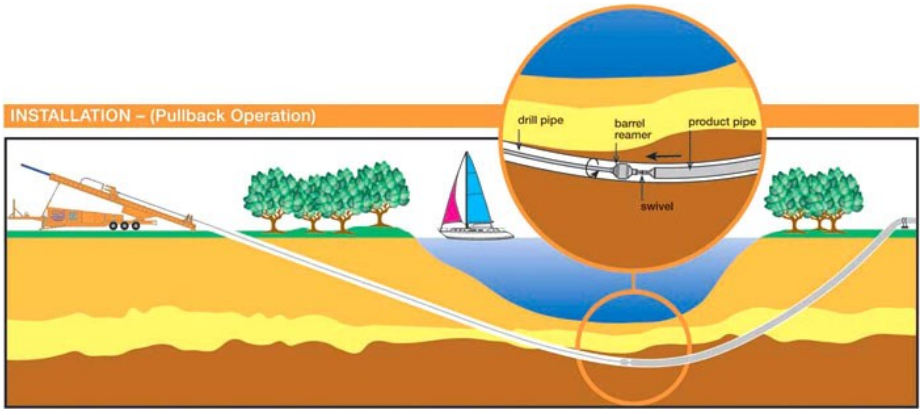

Figure 2.6. Pullback operation in HDD (Courtesy of Trackson Horizontal Drilling Pty Ltd.)

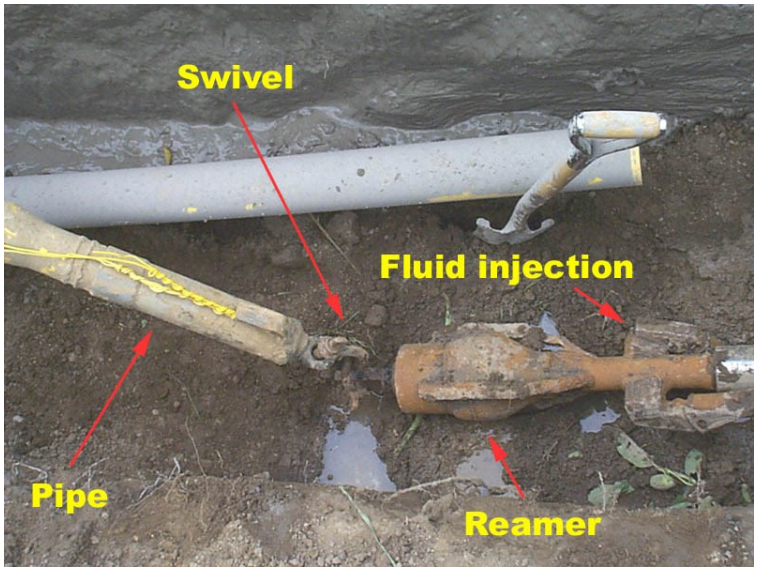

Figure 2.7. Components of pullback operation (Abraham and Gokhale, 2002)

The pipeline should be supported on the ground by rollers or cranes to prevent damages to pipe or its coating. It also reduces the friction on the ground and provides the required curvature to easier pull the pipeline down to the hole. Pipe materials are mostly high-density polyethylene (HDPE). Steel, Polyvinyl-chloride (PVC), and ductile iron are the other types of pipe material used in HDD.

2.1.4. Drilling Mechanics Data

As discussed earlier, boring a hole is accomplished by applying a combination of a forward thrust, rotary torque and the impact pressure of the drilling fluid. A successful HDD operation depends on safe application of all mechanical and hydraulic drilling parameters. For instance, one of the major risks during an HDD process is the inadvertent drilling fluid return. During normal condition, it is expected that drilling fluid which is pumped down to the hole, flows back to the

surface. However, if the drilling mud pressure in the annulus exceeds the amount of maximum tolerable pressure by the soil, hydraulic fracturing of soil (frac-out) will occur and it will lead to dispersal of the drilling mud into surroundings environment and loss of circulation. Therefore, drilling mud pressure along with other parameters should be constantly checked by the personnel during the operation. There are a number of sensors to measure drilling parameters such as thrust, rotary speed, torque, ROP, pump rate, mud pressure and many other items. All of this information is recorded by an Electronic Data Recorder (EDR) and the operator monitors them during the process. Figure 2.8 shows an example of EDR screen displayed to the operator.

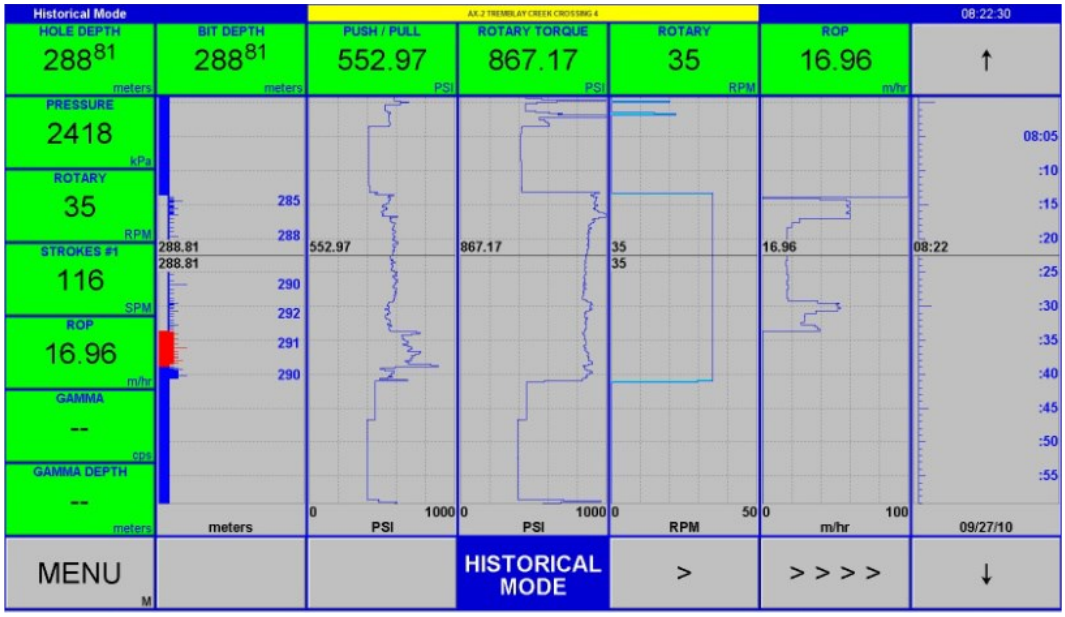

Figure 2.8. An EDR screen displayed to the operator

EDR provides both numerical and trace format for easier surveillance and it is customizable in terms of which parameter to be displayed. A skilled driller uses

each individual logs as a trending tool to avoid drilling problems and potential risks such as frac-out.

2.2. Fluidic Drag Estimation by Current Design Practices

Fluidic (viscous) drag is one component of the pullback load and it is the resistance to the pipe movement due to the slurry flow in the borehole. It results from the viscous shear stress on the outer surface of the pipe, which is created by the interaction between the viscous fluid and the pipe within the bore. There are several models to estimate the HDD pulling load for pipe installation, but calculation of the fluidic drag component has been a source of debate in all of them as explained hereafter.

Driscopipe (1993) is a simple approach to calculate the maximum pull load exerted on the pipe. This model treats the HDD drill path as a series of straight segments linked together and it considers friction and buoyancy weight into the calculation (Baumert and Allouche, 2002). But the fluidic drag is assumed to be negligible by this method.

Drillpath (1996) is a computer software program which is used for 3D design and construction of HDD profiles. This software computes the maximum tensile load during pipe installation by replacing the pipe with short elements. The summation of axial loads for each element gives the maximum pullback load. Again, this software does not consider the fluidic drag in its calculations.

ASTM F1962 (ASTM, 1999) is a standard for polyethylene pipe or conduit installation in HDD projects. It presents a series of equations to calculate the pullback load based on an idealized HDD profile which is shown in Figure 2.9. To calculate the fluidic drag, it assumes hydrokinetic pressure acting on the fluid, which is balanced by equal shear forces acting on the pipe and the borehole. Therefore, the fluidic drag (F_{HK}, N) is calculated as follows:

$$F_{HK} = \Delta p \frac{\pi}{8}(D_{bh}{}^2 - D_p{}^2) \tag{2.1}$$

Where D_{bh} is the borehole diameter, m; D_p is the pipe diameter, m; and Δp is hydrokinetic pressure, Pa. ASTM F1962 suggests a value of 70 kPa (10 psi) for hydrokinetic pressure; however, the Plastic Pipe Institute (PPI, 2009) assumes a range for hydrokinetic pressure between 30 to 60 kPa (4 to 8 psi). ASTM F1962 does not consider the length of the installed pipe, and it predicts lower fluidic drag in a tighter annulus; conversely, it gives higher values for larger annular areas, which is not consistent with the field observations (Duyvestyn, 2009). Moreover, assuming a constant Δp for all type of drilling fluids and annular geometries limits the correct description of slurry flow in HDD.

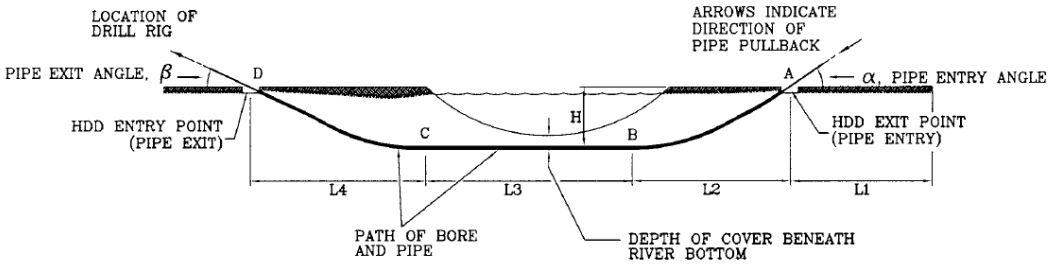

Figure 2.9. A simplified HDD profile (ASTM F1962-11)

The Pipeline Research Council International (PRCI) presents a method to analyze the installtion loads and predict the maxmium HDD pulling load required for steel pipe installtions (Huey et al., 1996; Hair et al., 2008). In PRCI model, the fluidic drag is treated as the friction force between the slurry and the pipe, and it is estimated by a mud coefficient of friction multiplied by the external area of the pipe, as follows:

$$Drag = \mu_{mud} \pi D_p L \tag{2.2}$$

Where *Drag* is the fluidic drag, N; μ_{mud} is the mud coefficient of friction, Pa; D_p is the pipe diameter, m; and L is the length of the pipe in the borehole, m. The fluidic drag coefficient is the typical viscous shear stress on a steel pipe pulled through a betonite viscous fluid, which has a value of 345 Pa (0.05 psi) as recommended by the Dutch Pipeline Standard NEN 3650 (NEN, 1992). Further comparisons between predicted pullback loads and actual field data conducted by Puckett (2003) resulted in a lower drag coefficient of 172 Pa (0.025 psi). However, assuming a constant shear stress on the pipe as μ_{mud} is not a correct assumption, since it is indeed a funtion of drilling fluid rheology, annular geometry (pipe and bore diameters), and the flow rate.

2.3. The Concept of Specific Energy in Drilling

The concept of Specific Energy (SE) was first introduced by Teale (1965) and he defined it as the energy required to excavate a unit volume of rock. He mentioned that the input energy for drilling was provided by the axial and torsional work done

by the drill bit. The axial work done in a unit time is given by multiplying the force by the penetration distance per unit time which is ROP:

$$\text{Axial Work} = F.ROP \tag{2.3}$$

Where, F is the thrust, N; and ROP is the rate of penetration, m/s. Torsional work in a unit time is the product of applied torque and the perimeter of the circle of rotation and number of revolutions and is given by:

$$\text{Torsional Work} = 2\pi.N.T = 2\pi.N.T \tag{2.4}$$

Where, N is the rotary speed, revolution/s; and T is the torque, N-m. The excavated volume per unit time is given by the product of ROP and the area of the drill bit (A_b, m^2) as:

$$\text{Excavation Volume} = A_b.ROP \tag{2.5}$$

The equation for specific energy is then derived by dividing the total input works by the output volume of excavation per unit time:

$$e = \frac{\text{Axial Work} + \text{Torsional Work}}{\text{Excavation Volume}} = \frac{F}{A_b} + \frac{2\pi.N.T}{A_b.ROP} = e_t + e_r \tag{2.6}$$

$$e_t = \frac{F}{A_b} \tag{2.7}$$

$$e_r = \frac{2\pi.N.T}{A_b.ROP} \tag{2.8}$$

Where, e is the SE, Pa; and subscripts t and r refer to the thrust and rotary components of the SE, respectively. SE has a dimension identical to stress or pressure which is force divided by area. Teale noticed that SE was mainly dependent on the nature of the rock and a relatively constant minimum amount of

energy is required to excavate in a given rock. The difference between this minimum energy and real drilling energy arises from energy losses in the system. Breaking the rock into smaller particles than necessary, and losses due to the friction between drilling tools are amongst the causes for higher amount of energy consumption in real processes. Teale realized from lab drilling data that the minimum amount of energy for a given rock is equal to the rock compressive strength. Based on this, he defined the mechanical efficiency of drilling (EFF_M) by dividing the minimum required specific energy to the actual energy consumption (e_{real}):

$$EFF_M = \frac{\text{Min. Specific Energy}}{e_{real}} = \frac{\text{Rock Compressive Strength}}{e_{real}} \qquad (2.9)$$

This definition was very useful from an operational point of view because it provided a reference point for efficiency and it developed a tool for determining bit performance and measuring the efficiency of the drilling process. Rabia (1985) used this concept as a criterion for bit selection based on measuring the bit efficiency and cost per foot of drilling. He showed that SE can be used for planning the drilling cost of a well and it is a meaningful criterion for ending the use of a current bit. Waughman et al. (2002) addressed one of the important decision making process that affected the efficiency of well drilling and that was when to replace worn bits. They used real-time SE monitoring to optimize the point when it was needed to pull a bit and they showed that it was leaded to substantial cost savings to replace a bit as soon as the SE level increased to a predetermined cut-off level.

Concept of SE became a key element for Fast Drill Process (FDP) which is a process to drill with the highest possible ROP in terms of technical and economical aspect. In early 2004, Exxon Mobile Corp. added a real-time display of SE to their drilling system in six rigs based on the surface measurements to determine if the concept was useful for their rig personnel to optimize drilling rates (Dupriest and Koederitz, 2005). In a period of three months, they succeeded to increase ROP by 133% and established new field records. They demonstrated functional understanding of SE behaviour by varying WOB, bit rotational speed and hydraulics during drilling process to obtain higher ROP and observing the energy response. Weight on Bit (WOB) is the total amount of downward thrust exerted on a bit by the weight of the drill stem. They identified three different regions of a bit performance as it is shown in Figure 2.10.

In region 1, bit performance is inefficient because of inadequate depth of cut available for the bit due to the low amount of WOB. The amount of SE used by the bit is high and ROP is low for region 1. Region 2 represents the segment where the bit functions in its maximum efficiency and an increase in WOB results in a linear growth in ROP. For this part, SE is at its lowest value and it remains constant regardless of changes in drilling parameters. They observed that drill bits at their peak efficiency transferred only 30-40% of their input energy to destroy the rock. Because they saw that the original equation gave values around three times of rock compressive strength while the bit was operating in efficient region. Therefore, they modified Teale (1965)'s concept by multiplying the Eq. 2.6 by bit efficiency factor

of 0.35. In region 3, the bit performance enters another area of inefficiency due to the development of a condition which limits the transfer of energy from the bit to the rock. The point where the ROP stop responding linearly with increasing WOB is called founder point. Vibration, bit balling (due to the accumulation of materials on the cutting structure of drill bit), and bottom hole balling (due to the accumulation of materials on the bottom of the hole) are common reasons for foundering. In this region, energy consumption begins to rise which is an indicator for occurrence of an inefficiency condition.

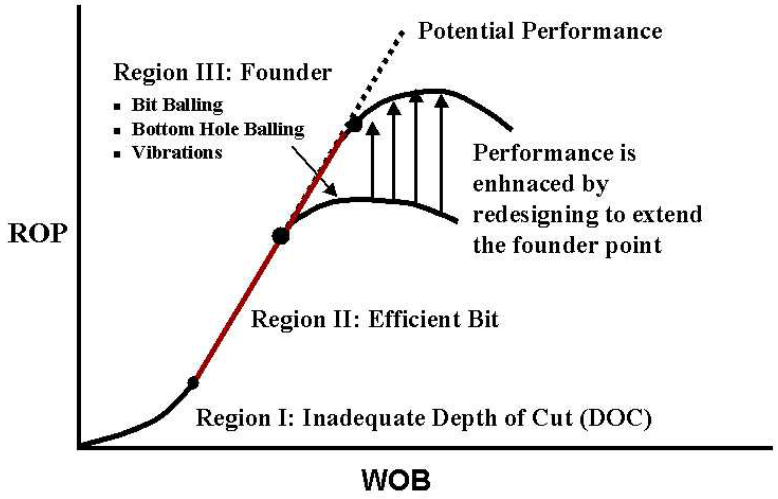

Figure 2.10. Relationship between ROP and WOB (Dupriest and Koederitz, 2005)

Filed tests by Dupriest and Koederitz (2005) showed that the length of region 2 in Figure 2.10 could be extended by using higher hydraulic horsepower per square inch of the drill bit (HSI). They mentioned that drilling hydraulics can be adjusted to get a desired ROP for a given bit and formation. The importance of bit hydraulics

on drilling efficiency was also reported earlier by Pessier and Fear (1992). Figure 2.11 demonstrates how faster drill rate is resulted from higher HSI.

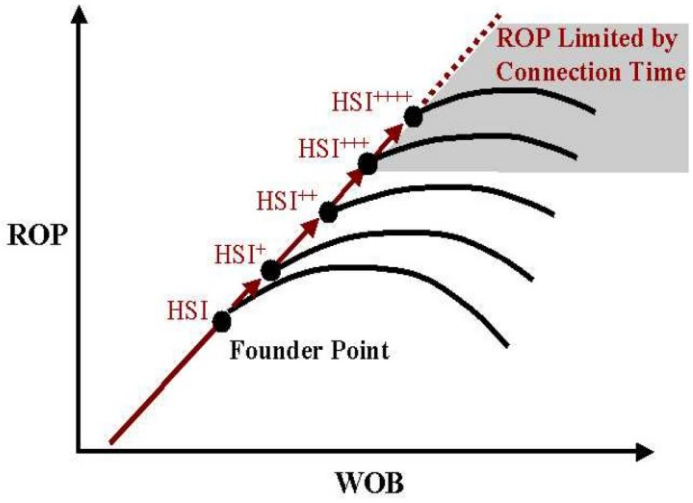

Figure 2.11. Drilling hydraulics can be adjusted to get a desired ROP (Dupriest and Koederitz, 2005)

SE surveillance proved to have the ability to detect changes in efficiency of the drilling process and improve the bit performance. Koederitz and Weis (2005) concluded that minimizing the value of SE is a good rule of thumb for adjusting drilling parameters. Caicedo et al. (2005) successfully predicted ROP for a given bit by using real-time SE surveillance. They also measured the torque and rotary speed required to achieve a desired ROP for a given bit and rock type. Later, Dupriest (2006) mentioned that ROP management process based on SE surveillance had been expanded to two thirds of Exxon Mobile teams worldwide, drilling 4.5 million feet of hole annually and it was going to be implemented to the remainder of the operator's rigs by the end of the same year. He reported the results of

performance improvement for six different teams compared from their recent performance without SE surveillance in Figure 2.12.

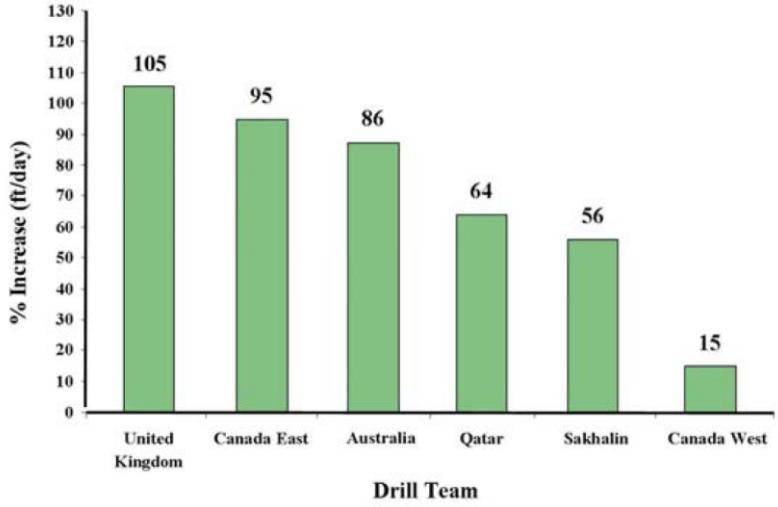

Figure 2.12. Performance increase gained by ROP management process (Dupriest, 2006)

Based on the significant gains in improving drilling efficiency by monitoring energy, SE became a standard trending tool in the logging system of the drill rigs. Remmert et al. (2007) claimed that USD 54 million had been saved while drilling 143 km (470,000 ft) in Qatar by using SE surveillance. They also reported 50 new drilling records and set one of the best safety records by 2006.

Experimental tests had shown the importance of bit hydraulics in ROP optimization but no attempt had been made to incorporate the hydraulic energy into the SE concept. Armenta (2008) added a bit hydraulic term to the SE equation and named the new concept as Drilling Specific Energy (DSE). DSE was defined as the work done to excavate a unit volume of rock and remove it from underneath the bit. He mentioned that the new equation could successfully identify inefficient drilling

conditions and the three regions of bit performance. Figure 2.13 shows the connection between the traditional graph for bit performance and new DSE vs ROP correlation.

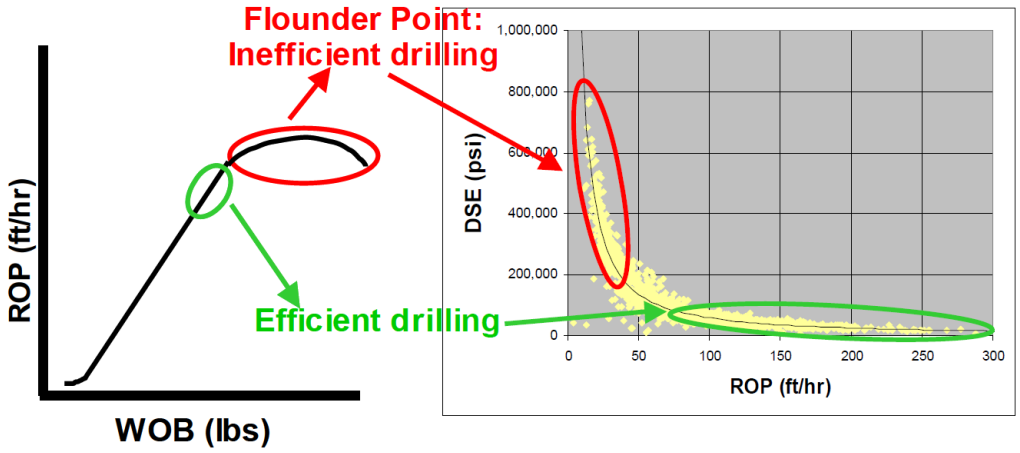

Figure 2.13. The connection between the traditional graph for bit performance and DSE vs ROP correlation (Armenta, 2008)

Based on his experimental data, DSE used by the bit matched the rock compressive strength during optimum condition. He mentioned that bit HSI is the main factor to move from inefficient drilling to the efficient region when WOB is constant. DSE equation is given in field units as:

$$DSE = \frac{F}{A_b} + \frac{120\pi.N.T}{A_b.ROP} - \frac{1{,}980{,}000\lambda.HP_b}{A_b.ROP} \qquad (2.10)$$

Where, DSE is the drilling specific energy in psi; N is in revolution/min; T is in lb-ft; A_b is in in.^{2}; ROP is in ft/hr; λ is a dimensionless bit-hydraulic factor depending on bit diameter, HP_b is bit-hydraulic power in hp; and 1,980,000 is a unit conversion factor.

Mohan et al. (2009) introduced a comprehensive set of equations to incorporate hydraulics into the Teale (1965)'s original equation. They mentioned that to correctly match the required specific energy to the strength of material being drilled, hydraulic energy should not be separated from the mechanical energy of drilling. Hydraulics is required to remove the cuttings and transfer them away from the bit and for the case of very soft formation, jet impact energy accomplishes the destruction process without any contribution needed from the mechanical work. They investigated several filed studies and showed that efficiency analysis was more accurate when considering the total energy involved in drilling which they called it Hydro-Mechanical Specific Energy (HMSE). HMSE was defined as the total amount of energy required to excavate and remove a unit volume of material from the cutting face. Jet impact impingement caused by the drilling fluid, forward thrust, and rotary torque are the input energies for the drill bit to bore a hole. In the present study, HMSE is briefly called SE and used as the concept to consider the total energy of drilling in HDD and it is obtained as follows:

$$e = \frac{F}{A_b} + \frac{2\pi.N.T}{A_b.ROP} + \frac{\eta.\Delta p_b.Q}{A_b.ROP} \tag{2.11}$$

Where, e is the SE, Pa; η is an energy reduction factor; Δp_b is the pressure drop across the bit, Pa; and Q is the volumetric flow rate, m^3/s.

2.4. Conclusions

HDD is the most rapidly growing technique amongst trenchless methods due to its environmentally friendly procedure and wide range of application. However,

examination of HDD process requires more attentions from engineers to better predict the required pipe pulling loads and more efficient drilling operations. The lack of a reliable method to predict fluidic drag during HDD becomes clear when a review of available HDD design practices shows several conflicts in their approaches to calculate fluidic drag.

A review of the concept of specific energy was done here to demonstrate how it can be implemented in HDD. Eq. 2.11 is going to be used in chapter 4 to calculate SE in HDD including hydraulic work as well as mechanical work done by the drill bit. Successful implementation of SE in oil field and the similarity of HDD drilling process to the oil well drilling indicate promising application of SE in HDD.

3. Chapter 3: Fluidic Drag Estimation in Horizontal Directional Drilling Based on Flow Equations[1]

3.1. Introduction

Horizontal directional drilling (HDD) is a rapidly growing trenchless method used to install new utilities without the environmental hazards and urban disruptions associated with traditional cut and cover methods (Najafi, 2014). Consequently, HDD is a preferred technique for utility installation beneath structures, roadways, lakes, rivers, and environmentally sensitive areas. The process begins with drilling a small bore, called pilot hole. Once the drill bit emerges from the exit point and the pilot hole is completed, the next step is to ream the hole. The reaming process may be skipped for installations with smaller pipe diameters, or may require several passes until the desired borehole diameter is acquired. The final step is the pipe installation, where the product pipe is pulled down into the bore. The pulling force applied to the pipe during this stage is an important parameter for design.

Estimation of the pipe pullback load is crucial for design engineers during planning stages of HDD operations to select the appropriate product pipe and rig size. The product pipe should have adequate strength to avoid damages during

[1] A version of this chapter has been submitted to the ASCE Journal of Pipeline Systems Engineering and Practice.

installation while the drilling rig should be capable of providing the required load to pull the pipe. Pullback force is a function of several factors, including the net buoyancy weight of the pipe in the borehole, the frictional forces, and the fluidic drag (Baumert et al., 2002). Various methods have been proposed to predict the pullback load, each approaching the fluidic drag component differently (Driscopipe, 1993; Drillpath, 1996; Huey et al., 1996; ASTM, 1999; Polak et al., 2002). Poor agreements of these methods by the field measurement suggest the need for development of comprehensive models that better reflect the reality of pipe installation using HDD (Duyvestyn, 2009; Baumert et al., 2002). Discordant predictions for fluidic drag by current design procedures have revealed the significance of having a reliable method for calculation.

In this chapter, current methods for estimating fluidic drag are reviewed, and a new approach for calculating fluidic drag is proposed based on the mechanics of drilling fluid. Then, a case study is investigated to compare fluidic drags calculated based on different models. Finally, a sensitivity analysis is performed to investigate the impact of various parameters on fluidic drag.

3.2. Current Methods for Predicting Fluidic Drag

Fluidic (viscous) drag is the resistance to the pipe movement due to the slurry flow in the borehole. It results from the viscous shear stress on the outer surface of the pipe, which is created by the interaction between the viscous fluid and the pipe within the bore. As cited above, there are several methods to estimate the HDD

pulling load for pipe installation, but calculation of the fluidic drag component has been a source of debate in all of them as explained hereafter.

In early models of pullback force estimation, such as Driscopipe (1993) and Drillpath (1996), the fluidic drag is assumed to be negligible. ASTM F1962 (ASTM, 1999) is a standard for polyethylene pipe or conduit installation in HDD projects. To calculate the fluidic drag, it assumes hydrokinetic pressure acting on the fluid, which is balanced by equal shear forces acting on the pipe and the borehole. Therefore, the fluidic drag (F_{HK}, N) is calculated as follows:

$$F_{HK} = \Delta p \frac{\pi}{8}(D_{bh}{}^2 - D_p{}^2) \tag{3.1}$$

Where D_{bh} is the borehole diameter, m; D_p is the pipe diameter, m; and Δp is hydrokinetic pressure, Pa. ASTM F1962 (ASTM, 1999) suggests a value of 70 kPa (10 psi) for hydrokinetic pressure; however, the Plastic Pipe Institute (PPI, 2009) assumes a range for hydrokinetic pressure between 30 to 60 kPa (4 to 8 psi). ASTM method does not consider the length of the installed pipe, and it predicts lower fluidic drag in a tighter annulus; conversely, it gives higher values for larger annular areas, which is not consistent with the field observations (Duyvestyn, 2009). Moreover, assuming a constant Δp for all type of drilling fluids and annular geometries limits the correct description of slurry flow in HDD.

The Pipeline Research Council International (PRCI) presents a method to analyze the installtion loads and predict the maxmium HDD pulling load required for steel pipe installtions (Huey et al., 1996; Hair et al., 2008). In PRCI model, the fluidic drag is treated as the friction force between the slurry and the pipe, and it is

estimated by a mud coefficient of friction multiplied by the external area of the pipe, as follows:

$$Drag = \mu_{mud} \pi D_p L \tag{3.2}$$

Where *Drag* is the fluidic drag, N; μ_{mud} is the mud coefficient of friction, Pa; D_p is the pipe diameter, m; and L is the length of the pipe in the borehole, m. The fluidic drag coefficient is the typical viscous shear stress on a steel pipe pulled through a betonite viscous fluid, which has a value of 345 Pa (0.05 psi) as recommended by the Dutch Pipeline Standard NEN 3650 (NEN, 1992). Further comparisons between predicted pullback loads and actual field data conducted by Puckett (2003) resulted in a lower drag coefficient of 172 Pa (0.025 psi). However, assuming a constant shear stress on the pipe as μ_{mud} is not a correct assumption, since it is indeed a funtion of drilling fluid rheology, annular geometry (pipe and bore diameters), and the flow rate. The influence of different parameters on fluidic drag will be discussed later.

Overview of current models indicates that they have used different assumptions to simplify the viscous drag calculation and they have not considered all of the important factors which affect the drag inside the borehole. The key to an accurate prediction of fluidic drag relies on fluid mechanics of the drilling mud within the annulus.

3.3. Fluid Mechanics of Drilling

Fluidic drag acting on the pipe can be calculated using rheological models for the flow of the drilling slurry. Rheology is the science to explain how fluids flow. To model rheology of a drilling fluid, the first step is to understand viscosity. In order to define viscosity, assume that there is a fluid between two parallel plates under steady state condition. If a force (F) is applied to the upper plate, moving it with a constant velocity, the shear stress ($\tau_{yx}=F/A$) is applied to the fluid, in which A is the contact area between the plate and the liquid, as illustrated in Figure 3.1.

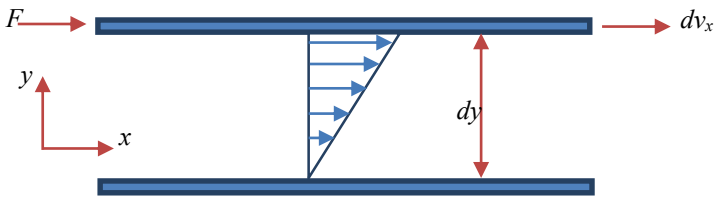

Figure 3.1. Schematic of a shearing flow (Chhabra and Richardson, 1999)

The shear stress causes a velocity profile in the fluid ranging from the upper plate's velocity in the top layer to zero at the bottom. The shear strain rate (shear rate) ($\dot{\gamma}_{yx}$) results from the changing velocity (dv_x) amongst the differing layers of the liquid, which is defined as (Chhabra and Richardson, 1999):

$$\dot{\gamma}_{yx} = \frac{dv_x}{dy} \tag{3.3}$$

The first subscripts on τ and $\dot{\gamma}$ refers to the direction normal to that of shearing force and the second subscripts shows the direction of the flow. Then, the ratio of the shear stress to the shear rate is defined as viscosity (μ):

$$\mu = \frac{\tau_{yx}}{\dot{\gamma}_{yx}} \tag{3.4}$$

3.3.1. Newtonian and non-Newtonian models

By changing the applied force exerted to the plate in Figure 3.1, the shear stress and the shear rate will also change. In Newtonian fluids, Eq. 3.4 is valid for all different ranges of shear stress and shear rate for a given temperature and pressure. Therefore, a plot of shear stress versus shear rate, called a "flow curve", is linear and passes through the origin. Non-Newtonian fluids are those in which the value of shear stress divided by shear rate is inconstant, and their flow curve is not linear or does not pass through the origin.

Different rheology models have been developed to describe fluid behavior. For simplicity, some researchers use the Newtonian model to approximate fluid behavior in HDD (Polak et al., 2002; Chehab et al., 2008). However, drilling muds are classified as non-Newtonian fluids due to the interactions between the fluid and solid particles in the slurry. Bingham plastic and Power Law are the most common non-Newtonian models used in the HDD industry (Baroid, 1998). Osbak (2011) suggested that Power Law model is more accurate for modeling drilling fluid in HDD, which is also the model used to calculate fluidic drag in this chapter.

Power Law model introduced by Ostwald (1925) and it assumes the following relationship between shear stress and shear rate:

$$\tau = K\dot{\gamma}^{n} \tag{3.5}$$

Where K is the fluid consistency coefficient, and n is the flow behaviour index. For the flow behaviour index less than one, the apparent viscosity of a fluid decreases with increasing shear rate and the fluid shows shear-thinning or pseudoplasticity properties. The fluid exhibits shear-thickening behaviour when Power Law behaviour index is greater than unity. Only pseudoplastic fluids are used to model drilling muds because shear-thickening fluids are very rare and very limited reliable data have been reported about this type of behaviour (Chhabra and Richardson, 1999). The consistency coefficient of the fluid represents the fluid pumpability or overall thickness (Ariaratnam et al., 2007). The unit of the consistency coefficient depends on the value of the behaviour index and it has units such as dyne-s^n/cm^2 and Pa-s^n. Equations for the annular flow of the drilling mud in HDD based on Power Law model are presented hereafter.

3.3.2. Annular Flow

During HDD process, the borehole is always filled with a drilling mud, which functions to stabilize the bore, cool and lubricate the drilling equipment, transfer cuttings to the surface, increase the rate of penetration, and fill the annulus after the product pipe is installed (Ariaratnam et al., 2007). The drilling fluid is consistently pumped into the borehole during the HDD process. Therefore, there should be a pressure gradient in the borehole for the slurry to flow.

Modeling axial flow of fluid through an annulus is of a great importance to industries such as oil and gas explorations and HDD. Calculation of flow rate, pressure gradient, shear stress, and velocity profile are required in design of

processes and equipment. Here, it is needed to calculate the shear stress at the wall of the pipe to predict the viscous drag. Therefore, some simplifying assumptions are used for fluid mechanics of the drilling mud. The flow regime is assumed to be laminar in which the layers of fluid moves parallel to each other. It is also assumed that the drilling mud is incompressible, and the system is isothermal and free of gravity. Idealizing the mud flow in the borehole is necessary for a quantitative description of the annular flow. However, in reality, there are other significant factors affecting the flow pattern in the annulus. For example, the borehole wall may vary considerably from a circular shape and the above-mentioned models do not consider the time-dependent behaviour of fluids (Mitchell and Miska, 2011).

Another important reallity of annular flow in HDD is the fact that the pipe is eccentric over the most of the borehole. Eccentricity happens when the centerlines of the pipe and the borehole do not coincide. For a concentric annulus, the flow is uniform around the pipe while eccentricity causes a predominant flow regime in the widened section and a stagnant region in the narrowing area of the annulus (Haciislamoglu and Langlinais, 1991). This uniformity in eccentric flow results in a considerable change in velocity profile and shear stress distribution around the pipe and their exact predictions are too complicated to be made by an industry-friendly method. Numerical model by Haciislamoglu and Langlinais (1990) showed that for a constant flow rate, the frictional pressure loss decreases with increasing eccentricity. Therefore, a concentric annulus is conservatively assumed here to describe the flow of the drilling mud in HDD process.

For the laminar flow of a Power Law fluid through the space between two coaxial cylinders (Figure 3.2), the shear stress is given by (Fredrickson and Bird, 1958):

$$\tau_{rz} = \frac{R}{2}\frac{(-\Delta p)}{L}\left(\xi - \frac{\lambda^2}{\xi}\right) \tag{3.6}$$

Where τ_{rz} is the shear stress at radius r from the centerline of the bore, R is the borehole radius, $\Delta p/L$ is the pressure gradient, $\xi = r/R$ is the normalized radius, and λ is the location of maximum velocity (at $r = \lambda R$), as shown in Figure 3.2. The value of the pressure gradient is negative in flow direction, so $-\Delta p/L$ is used as the positive value of the pressure gradient.

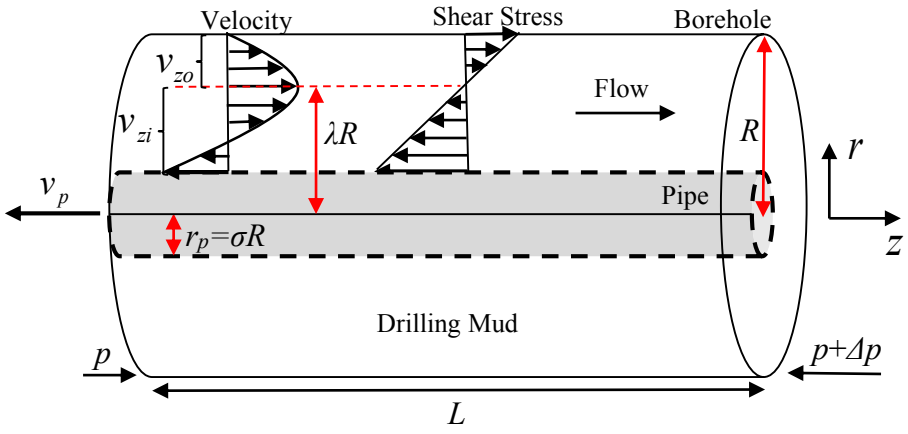

Figure 3.2. Flow in a concentric annulus

The velocity of the slurry is given by applying the Power Law rheology equation to Eq. 3.6. To account for sign changes of the shear rate in the annulus, the Power Law model can be rewritten as:

$$\tau_{rz} = -K\left|\frac{dv_z}{dr}\right|^{n-1}\frac{dv_z}{dr} \tag{3.7}$$

Then, the velocity of the fluid is obtained by substituting Eq. 3.7 into Eq. 3.6, and integrating with respect to velocity. Boundary conditions are $v=-v_p$ at $r=r_p$ and $v=0$ at $r=R$ where r_p and v_p is the pipe radius and pullback speed, respectively. The velocity profile in the annulus is given as:

$$v_{zi} = -v_p + R\left(\frac{R}{2K}\frac{-\Delta p}{L}\right)^{1/n}\int_{\sigma}^{\xi}\left(\frac{\lambda^2}{x}-x\right)^{1/n}dx \qquad \sigma \le \xi \le \lambda \tag{3.8}$$

$$v_{zo} = R\left(\frac{R}{2K}\frac{-\Delta p}{L}\right)^{1/n}\int_{\xi}^{1}\left(x-\frac{\lambda^2}{x}\right)^{1/n}dx \qquad \lambda \le \xi \le 1 \tag{3.9}$$

Where $\sigma=r_p/R$, and v_{zi} and v_{zo} are the fluid speed within the inner and outer region of annulus, respectively as shown in Figure 3.2. The values of λ and $-\Delta p/L$ are unknown in Eq. 3.6, 3.8 and 3.9. To find these unknowns, a system of two equations is required. The first equation to solve for the unknowns is given by equating v_{zi} and v_{zo} at $\xi=\lambda$. The second equation of the system is obtained by writing the volumetric flow rate (Q) in terms of the fluid velocity in the annulus as:

$$Q = 2\pi R^2\int_{\sigma}^{1}\xi v_z d\xi \tag{3.10}$$

To simplify the equation given after substituting Eq. 3.8 and 3.9 into Eq. 3.10, an analytical solution similar to that proposed by Hanks and Larsen (1979) was used to evaluate the integral, and the final solution of Eq. 3.10 is obtained as:

$$Q = \frac{n\pi R^3}{1+3n}\left(\frac{R}{2K}\frac{-\Delta p}{L}\right)^{1/n}\left[(1-\lambda^2)^{1+1/n} - \sigma^{1-1/n}(\lambda^2-\sigma^2)^{1+1/n}\right]$$

$$+\pi R^2 v_p\left(\frac{1-n}{3n+1}\lambda^2+\sigma^2\right) \tag{3.11}$$

Now, λ and $-\Delta p/L$ can be evaluated by solving a set of two unknowns and two equations. Then, the shear stress at the wall of the pipe (τ_p) is given by Eq. 3.6, where $\xi = \sigma$:

$$\tau_p = \frac{R}{2}\left(\frac{-\Delta p}{L}\right)\left(\sigma - \frac{\lambda^2}{\sigma}\right) \tag{3.12}$$

The shear stress on the pipe during the installation operation in HDD can be calculated from the abovementioned flow equations. Finally, the fluidic drag on the pipe is obtained by multiplying the shear stress on the pipe by the pipe area, as follows:

$$T_d = 2\pi r_p \tau_p \tag{3.13}$$

Where T_d is the fluidic drag per unit length of the pipe.

3.4. Case Study

In this section, the proposed flow equations were used to calculate fluidic drag in a case study. The result was then compared with the fluidic drags predicted by PRCI and ASTM F1962. The installation of a 40-centimeter (16 in) pipe in a 560-meter (1850 ft) length river crossing using HDD in Alberta, Canada was investigated as the case study. Figure 3.3 shows the profile of the HDD crossing. The Power Law rheological parameters (K, n) were obtained by a six-speed rheometer using 100 and 3 rpm values. Table 3.1 presents the parameters used in fluidic drag calculations.

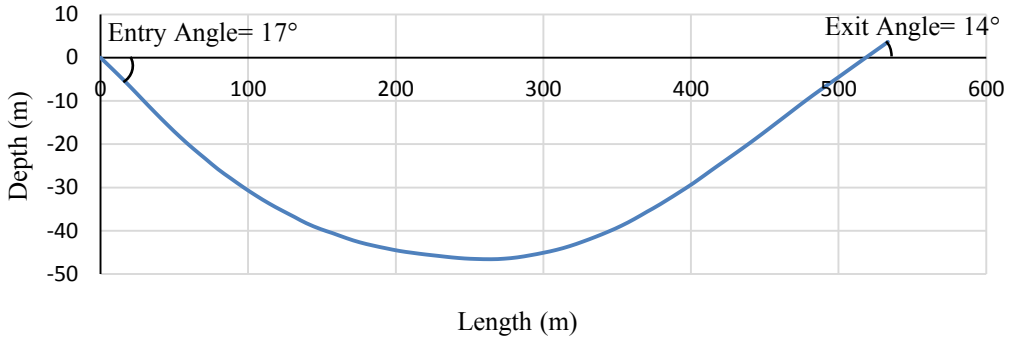

Figure 3.3. Profile of the HDD crossing

Table 3.1. Parameters of the HDD river crossing

Pipe diameter (m)	0.406 (16 in)
Hole diameter (m)	0.61 (24 in)
Pipe radius/hole radius, σ	0.67
Length of crossing (m)	560
Flow behavior index, n	0.35
Consistency coefficient, K (Pa.s^n)	4.02
Pipe speed (m/s)	0.01 (2 ft/min)
Discharge (m^3/min)	1.3

Figure 3.4 shows the fluidic drags predicted by different methods during the pipe installation. For comparison, drill rig pull load is also included in the graph which was measured during the operation by a sensor installed in between the swivel on the carriage and the drill pipe on the rig. It is worth noting that the pull load predicted by methods such as ASTM F1962 and PRCI is the load exerted to the product pipe, called the pullback load and fluidic drag is only one component of the pullback load. However, the rig pull load is the total load required to pull the

drill pipes and the reamer assembly inside the borehole in addition to the pullback load (Puckett, 2003).

As it can be seen from Figure 3.4, the fluidic drag calculated based on the proposed method began at zero, reaching 8% of the maximum rig load at the end of the installation. Fluidic drag by PRCI was singinficantly higher that those predicted by the other two methods and the maximum drag happened at the end of the river crossing since it is a function of the length of pipe within the hole. Using PRCI method for design and planning purposes may result in assumunig higher installation loads and imposing costly operation. For this case study, the fluidic component alone would suggest a maximum drag as large as the maximum rig load and it even exceeded the installation load at the final lengths of the pullback.

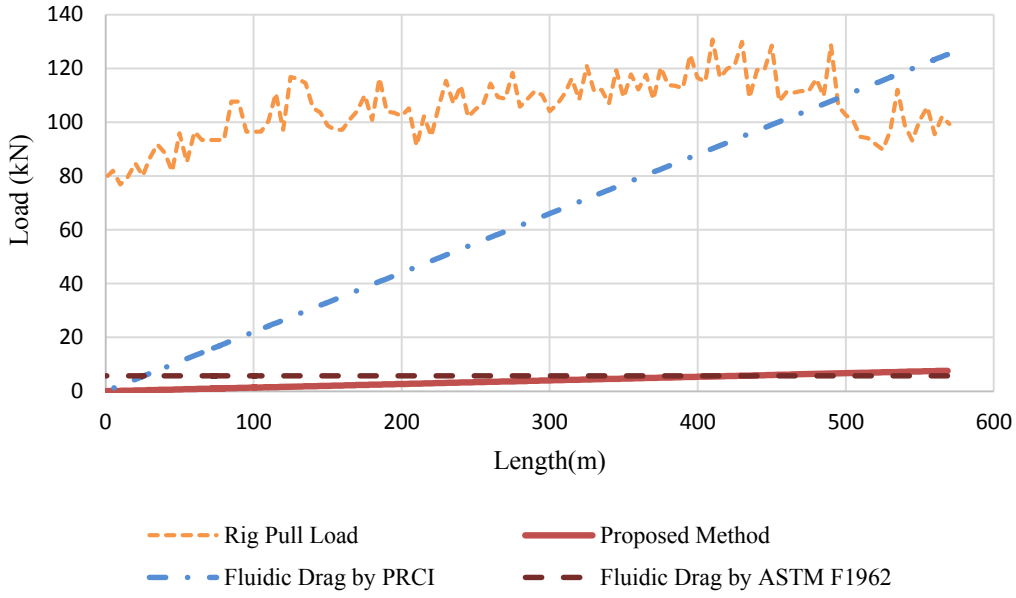

Figure 3.4. Fluidic drags calculated by different methods and their contribution to the measured rig pull load

Figure 3.4 indicates that ASTM F1962 predicted a constant drag for the whole length of the installation, since it does not consider the length of installed pipe within the borehole. However, among the two common methods, drag calculated by ASTM F1962 is closer to the maximum fluidic drag proposed by the flow equations. It should be noted that this case study is a typical HDD project with some typical design parameters. Hence, ASTM F1962 is not able to consider the effects of all design factors in drag, it would likely to understimate or overstimate the fluidic drag in different annular geomteris, hydrauilcs, and drilling mud rheological paramters.

3.5. Sensitivity Analysis on Parameters Affecting Fluidic Drag

A parametric sensitivity analysis is presented to investigate the effect of different parameters on fluidic drag during the pipe pulling stage. Rational ranges are considered for Power Law parameters, ranging from fresh drilling fluids (low slurry densities) to heavy slurries exiting the borehole. According to the Plastic Pipe Institute (PPI, 2009), the pipe speed installation ranges from 0.005 to 0.01 m/s (1 to 2 ft/min). To investigate the effect of pipe speed on fluidic drag, the immobile state of pipe is also considered (i.e. v_p=0). Various pipe sizes and ratio of pipe to borehole radii are considered to address the impact of annular geometry on fluidic drag. Table 3.2 presents the parameters and their variations.

Effective viscosity is used to better understand the changes in fluid consistency index (K) and the Power Law exponent (n). Effective viscosity is defined as the

viscosity of a fluid passing through a specific geometry and can be calculated for the Power Law model as (API, 1995):

$$\mu_{ea} = K\left(\frac{6v_{avg}}{R - r_p}\right)^{n-1}\left(\frac{2n+1}{3n}\right)^{n} \tag{3.14}$$

Where μ_{ea} is the effective viscosity, Pa; v_{avg} is the average velocity inside the annulus, m/s; K is fluid consistency index, Pa.s^n; and R and r_p are the borehole and the pipe radius, respectively, m. Table 3.2 indicates that moving from low to high values for n and K resulted in a more viscous drilling mud. However, the influence of the consistency index is much higher on the effective viscosity based on the defined ranges.

Table 3.2. Input parameters and their variations for the sensitivity analysis

Parameters	**Low**	←	**Ranges**		→	**High**	**Mean**
r_p (m)	0.1	02	0.3	0.4	0.5	0.6	**0.35**
r_p / R	0.4	0.5	0.6	0.7	0.8	0.9	**0.65**
v_p (m/s)	0	0.002	0.004	0.006	0.008	0.01	**0.005**
Q (gpm)	100	250	400	550	700	850	**475**
n	0.10	0.15	0.20	0.25	0.30	0.35	**0.225**
μ_{ea} (Pa)	3.19	3.36	3.49	3.61	3.72	3.82	
K (Pa.s^n)	1	2.5	4	5.5	7	8.5	**4.75**
μ_{ea} (Pa)	0.75	1.87	2.99	4.11	5.24	6.23	

A sensitivity analysis of fluidic drag with respect to each parameter was conducted for a reference set of mean values presented in Table 3.2. The percentage of change in fluidic drag was calculated when each parameter deviated from its

mean value. Changes in each parameter occurred while the other parameters were fixed in their mean. Figure 3.5a and b present the result of the analysis.

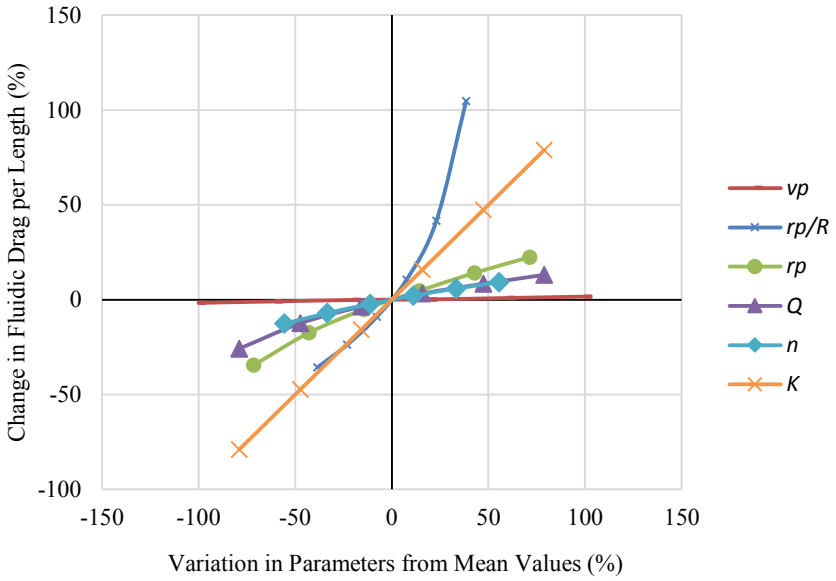

(a)

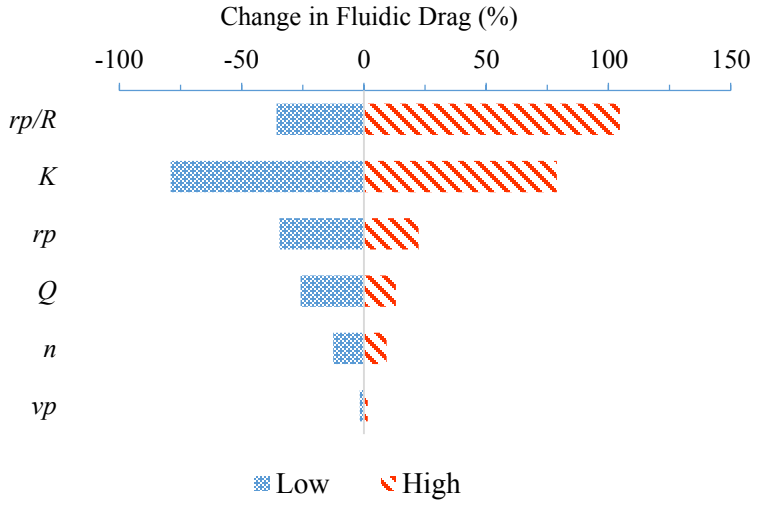

(b)

Figure 3.5. (a) Sensitivity analysis on fluidic drag per length with respect to different parameter. **(b)** Tornado diagram of parameters affecting fluidic drag during pullback

The results indicated that borehole to pipe radii ratio has the highest impact on fluidic drag. It is a common rule in HDD design to have a borehole diameter 1.5 times larger than the product pipe diameter (Ariaratnam and Allouche, 2000). Therefore, using a mean reference value of 0.65 for r_p/R is the current practice. Figure 3.5a indicates that increasing this value to 0.9 leads to an increase of over 100% in drag. This emphasizes the fact that larger load is required to pull the pipe within smaller annular areas. Therefore, engineers should consider this when they design a borehole with tighter annular area. It is also seen in Figure 3.5a that a change in the drag is more noticeable by increasing the ratio from the mean value in comparison with reducing the ratio. It indicates that assuming borehole diameter 1.5 time the pipe diameter provides optimum benefit and increasing the hole diameter beyond that value achieves less in terms of reducing drag.

Figure 3.5a also shows that higher drag can be encountered while pulling the pipe through a more viscous fluid. Greater values of *n* and *K* for drilling mud caused higher drag to be exerted on the pipe. The fluidic drag is more sensitive to *K*, since greater change in viscosity occurred when *K* was altered.

According to PRCI, pipe radius must have a linear relation with fluidic drag with a slope of unity. However, further analysis showed that increasing pipe size while the other parameters are fixed, results in smaller viscous shear stress on the pipe due to decreased frictional pressure loss in the annulus. Given the shear stress, the drag is obtained by multiplying the stress by the perimeter of the pipe.

Consequently, the resultant drag has a positive relation with the pipe radius, but change in pipe size does not result in the same amount of change to drag.

Figure 3.5a also demonstrates that the pullback speed has a low impact on fluidic drag in comparison with other parameters. The difference in fluidic drag when pullback speed is zero with when v_p=1 cm/s is less than 5%. Hence, the flow equations with no-slip boundary condition at the pipe's wall are simpler to use; it is easier to calculate fluidic drag without considering the pipe speed. For this case, all flow equations presented in this chapter can be used by setting v_p=0.

Figure 3.5b is a tornado diagram and it shows the order of significance of each parameter in fluidic drag from top to bottom in the y-axis and it demonstrates how the fluidic drag changes when each parameter moves from its mean to the lowest or highest value.

3.6. Conclusions

A new method was proposed to calculate fluidic drag exerted on the pipe during pullback stage in HDD. The flow equations for a Power Law fluid were developed to describe drilling slurry flow in the annulus. For a typical case study, the comparisons with measured rig pull load indicated that PRCI overestimated the fluidic drag excessively, while the fluidic drag calculated with the proposed method was about 8% of the maximum rig load. ASTM F1962 resulted in a closer prediction to the maximum drag calculated by the proposed model and it is

suggested to be used for fluidic drag estimation during design stage of an HDD process.

A sensitivity analysis was conducted over a wide range of rational values to investigate the impacts of different parameters on fluidic drag. The results revealed that the ratio of pipe to borehole radius has a dramatic effect on fluidic drag. The greater the ratio, the larger the load needed to overcome fluidic drag. Higher values of fluidic drag are expected while executing pullback in a more viscous fluid. Conversely, the speed of pullback does not affect the drag noticeably, and simpler flow equations can be used by setting v_p=0 in the abovementioned equations.

4. Chapter 4: Implementing the Concept of Specific Energy in HDD[2]

4.1. Introduction

Horizontal Directional Drilling (HDD) is used to drill long boreholes in the installation of utilities beneath surface obstacles such as rivers, lakes, roads, railways, and airport runways. HDD is a directionally controlled drilling method adopted from horizontal oil well drilling technology in the 1970's (Najafi, 2014). In a short period of time, HDD has been implemented worldwide and has turned into a multi-billion dollar industry (Sarireh et al., 2012). Expensive costs associated with drilling operations necessitate the need for the development of tools and methods to optimize the HDD process. Unlike aboveground construction projects, regular cost and risk reduction techniques cannot be used in HDD due to the existence of many uncertainties arising from unknown underground conditions. However, several methods have been developed to optimize the drilling process in the oilfield, which can benefit the HDD industry as well (Provost et al., 1987; Pessier and Fear, 1992).

A common technique used to reduce the time and risk of drilling projects is to optimize the rate of penetration (ROP). Extensive studies have been conducted

[2] A version of this chapter has been submitted to the ASCE Journal of Construction Engineering and Management.

intending to maximize ROP using new techniques or methodologies (Bourgoyne et al., 1973; Reed, 1972; Bonet et al., 1995; Wojtanowicz and Kuru., 1993). Drill operators have also conducted a range of tests to identify the maximum drill rates. For example, a "drill rate" test is one of the most common methods, which includes the analysis of various ROPs obtained by changing drilling parameters such as weight on bit (WOB) and rotational speed process (Dupriest and Koederitz, 2005). Then, the setting resulting in maximum ROP is selected for drilling operations. Another approach to optimize the drilling process is to analyze the amount of energy required to drill through the formation. The concept of Specific Energy (SE) has been used successfully in oil and gas drilling projects, and is one of the most efficient indicators of drilling operations. Energy surveillance helps to better understand the drilling mechanics and assists in the identification of downhole problems (Bevilacqua et al., 2013).

In this chapter, the principals of HDD operations and the concept of SE are reviewed, and a model is developed to compute the actual amount of energy used by the drill bit. Then, a case study is investigated as an example application of SE in HDD to provide a better understanding of how SE analysis can guide operators to avoid drilling problems and risks.

4.2. Review of Specific Energy in Drilling

The concept of SE was first introduced by Teale (1965), who defined it as the energy required to excavate a unit volume of rock. He stated that the input energy

for drilling was provided by the axial and torsional work done by the drill bit. The excavated volume per unit time is given when ROP is multiplied by the area of the drill bit. The equation for specific energy is then derived by dividing the input energy by the output volume of excavation per unit time:

$$e = \frac{\text{Axial Work} + \text{Torsional Work}}{\text{Excavation Volume}} = \frac{F}{A_b} + \frac{2\pi.N.T}{A_b.ROP} \tag{4.1}$$

Where e is the SE, Pa; F is the thrust, N; T is the torque, N-m; N is the rotational speed, revolution/s; ROP is the rate of penetration, m/s; and A_b is the bit area, m^2. SE has a dimension identical to stress or pressure, which is force divided by area. Teale (1965) noted that to excavate a unit volume of rock, a minimum energy equal to the rock's compressive strength was required. This amount of energy depends upon the nature of the rock and is therefore constant for each rock type. The difference between this minimum energy and the actual drilling energy arises from energy losses in the system. Higher amounts of energy consumption in the actual process can be due to the breaking of rock into smaller particles than necessary and the friction experienced between drilling tools. Therefore, maximum efficiency is achieved when drilling energy is close to the rock's compressive strength. Mechanical efficiency of drilling (EFF_M) is then derived by dividing the minimum required energy by the actual energy consumption (e_{real}):

$$EFF_M = \frac{\text{Min. Specific Energy}}{e_{real}} = \frac{\text{Rock Compressive Strength}}{e_{real}} \tag{4.2}$$

The concept of SE has become increasingly common as an efficiency indicator in the improvement of drilling operations. Dupriest and Koederitz (2005) optimized

drill rates by implementing SE surveillance in oil well drilling and adding a real-time SE calculator to the rig logging system. The authors categorized the bit performance in efficient and inefficient regions and observed that the maximum ROP could be achieved by varying the drilling inputs such as thrust, rotary speed, and hydraulic power while SE remained relatively constant at its minimum value. Koederitz and Weis (2005) concluded that minimizing the value of SE was a good principle for adjusting drilling parameters. Caicedo et al. (2005) successfully predicted ROP for a given bit by using real-time SE surveillance. They also measured the torque and rotary speed required to achieve a desired ROP for a given bit and rock type. Based on the significant improvement in drilling efficiency via energy monitoring, SE became a standard tool for rig personnel. Remmert et al. (2007) claimed that using SE surveillance in Qatar save approximately USD 54 million in a 143 km (470,000 ft) drilling project. The authors also reported 50 new fast drilling records along with one of the best safety records by 2006.

Further experiments show the importance of hydraulic energy in ROP optimization. Armenta (2008) added a drill bit hydraulic term to the concept of SE and demonstrated that the new equation could successfully identify inefficient drilling conditions. Mohan et al. (2009) concluded that to correctly match the required SE to the strength of material being drilled, hydraulic energy should not be separated from the mechanical energy of drilling. The authors investigated several field studies and showed that efficiency analysis was more accurate when it considered the total energy involved in drilling.

To increase the efficiency, SE should be kept as low as possible while drilling with the highest ROP. An increase in energy consumption indicates either a change in the rock formation type or an inefficiency condition such as bit wear, vibration, bit balling (due to the accumulation of materials on the cutting structure of drill bit), and bottom hole balling (due to the accumulation of materials on the bottom of the hole). All of these conditions limit energy transfer from the drill bit to the formation and result in lower ROP. Previous studies have proven that real-time monitoring of SE is a useful tool to evaluate bit performance and identify drilling problems (Guerrero and Kull, 2007; Pessier et al., 2012).

Successful implementation of the concept of SE in oilfield operations worldwide indicates that the HDD industry can also benefit from this efficiency indicator. This concept can provide HDD engineers with a powerful qualitative and quantitative tool to increase ROP. Moreover, SE surveillance is a useful tool for HDD operators to select the optimum combination of drilling parameters to drill as efficiently as possible.

4.3. Implementing SE in HDD

4.3.1. Real-time Drilling Data

A typical HDD borehole starts with an entry line aboveground, reaches a horizontal base line below ground surface, and then exits from an exit point on the surface. The length of the borehole ranges from 50 m to over 2000 m, and the depth below the surface varies from 3 m to 150 m (Osbak, 2011). There is a drilling rig

situated aboveground providing forward thrust and rotary torque for the drill bit to cut the materials and advance along the prescribed path. Drill pipes transmit the surface energy from the rig to the drill bit. A drilling fluid is pumped down to the borehole through the drill pipes and exits through the drill bit nozzles resulting in a jet impact force exerted on the bottom of the hole. The drilling mechanics data including thrust, rotary speed, torque, hydraulic parameters, and ROP are recorded during operations by the sensors on the drill rig. Therefore, a continuous real-time log records and displays drilling parameters for the operator (Figure 4.1). Conversion factors are used to change the pressure units of force and torque to their consistent units.

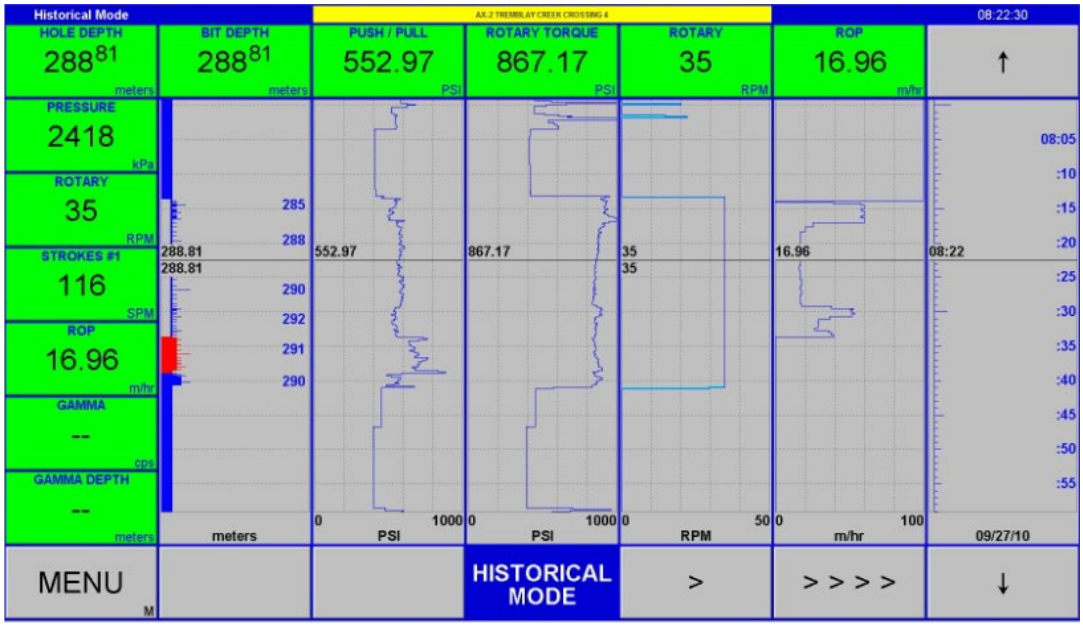

Figure 4.1. Drilling mechanics data displayed to HDD operator

The driller uses the displayed drilling data (Figure 4.1) as the indicators of the drilling condition. The factor of the operator's experience plays a very important

roll to the success of the operation. It is the driller's responsibility to continuously observe the drilling process and acquire the right information and adjust the rig drilling inputs based on his judgement. Therefore, two different drillers would likely use different techniques during the operation and this diversity in drilling process affects the productivity of HDD projects. However, the concept of SE can help the operator to better understand the process and identify the inefficiency conditions.

Real-time display of SE along with other drilling parameters on the operator's console provides rig personnel with a valuable trending tool and allows SE surveillance to be included in the operator's drilling practice. SE calculated using the recorded drilling data on the rig indicates the surface energy. However, not all the surface energy can be transferred to the drill bit due to the friction experienced by the drill pipes contacting the borehole and drilling fluid. Therefore, the effective energy available to the bit, called downhole SE, is less than surface SE due to the energy losses. Accordingly, a continual increase in surface energy during drilling at greater depths is inevitable. In lengthy HDD crossings, energy loss becomes considerable and surface SE analysis may lead to the assumption that the drill bit energy consumption is high and inefficient while the drill bit is actually running efficiently without using high energy. Therefore, prediction of the downhole SE is necessary to better describe the exact amount of energy spent by the bit.

To calculate the downhole SE, the thrust and torque should be measured downhole close to the drill bit. With the aid of sophisticated data acquisition tools,

it is possible to record downhole data during drilling operations (Bevilacqua et al., 2013). However, these expensive measurement tools may be economical for oil and gas industry, but they are too costly to be used in HDD projects. In an attempt to compare downhole and surface energies and to estimate the difference between them, an analytical model is proposed hereafter.

4.3.2. SE Equation in HDD

To consider the total energy required for drilling in HDD, a hydraulic term should be included along with the energy's axial and torsional components. Forward thrust, rotary torque, and jet impact impingement caused by the drilling fluid are the input energies required for the drill bit to bore a hole. The concept of specific energy proposed by Mohan et al. (2009) is used to relate all energy components in one equation and is defined as the energy required to excavate and remove a unit volume of material from the drill bit and it is obtained by adding the hydraulic energy term to Eq. 4.1 as follows:

$$e = \frac{F}{A_b} + \frac{2\pi.N.T}{A_b.ROP} + \frac{\eta.\Delta p_b.Q}{A_b.ROP} \tag{4.3}$$

Where e is the SE, Pa; η is an energy reduction factor; Δp_b is the pressure drop across the bit, Pa; and Q is the volumetric flow rate, m^3/s. SE has three components, namely thrust (e_t, Pa), rotary (e_r, Pa), and hydraulic energy (e_h, Pa):

$$e_t = \frac{F}{A_b} \tag{4.4}$$

$$e_r = \frac{2\pi.N.T}{A_b.ROP} \tag{4.5}$$

$$e_h = \frac{\eta.\Delta p_b.Q}{A_b.ROP} \tag{4.6}$$

Where e_t corresponds to the energy required to impose thrust and provide the bit with adequate depth of cut, e_r is the amount of energy consumed while rotating the drill bit and excavating materials, and e_h represents the hydraulic impact energy required to remove the cuttings and transport them away from the drill bit. As the drilling mud exits through the nozzles, an accelerated entrainment of the fluid occurs, causing only 25 to 40 percent of the jet energy to reach the face of the borehole (Warren 1987). Therefore, a reduction factor (η) was defined in the hydraulic energy component which can be computed for different drill bits. The reduction factor η is a function of the ratio of the nozzle jet velocity to the return velocity around the drill bit and the distance from the nozzle to the face of the borehole (Mohan et al., 2009).

Pressure drop across the bit is calculated as follows (Bourgoyne et al., 1991):

$$\Delta p_b = \frac{MW.Q^2}{2C_d{}^2.A_n{}^2} \tag{4.7}$$

Where MW is the mud weight, kg/m^3; A_n is the total nozzle area, m^3; and C_d is the nozzle coefficient. Substituting Eq. 4.7 into Eq. 4.3 gives a final equation for SE as:

$$e = \frac{F}{A_b} + \frac{2\pi.N.T}{A_b.ROP} + \frac{\eta.MW.Q^3}{2C_d{}^2.A_b.ROP.A_n{}^2} \tag{4.8}$$

4.4. A Model to Calculate Downhole SE

The thrust, the rotary speed, and the torque provided by the drill rig are transferred to the bit by means of the drill pipes. Drill pipes are extended from the entry point to the bit location at the bottom of the hole and are subjected to different loads during operations. These loads are divided as frictional force between the drill pipe and borehole, gravity load due to the weight of the drill pipe, and viscous force between the drill pipe and drilling fluid. The resistant torques limiting free rotation of the drill pipe within the borehole include the frictional torque due to tangential friction at the point of contact between the drill pipe and the borehole, and the viscous torque due to drill pipe rotation in a viscous fluid.

The proposed method requires the drill path to be subdivided into small, straight elements, with each element located between other straight elements (as shown in Figure 4.2). Calculation begins with the first element of the drilling trajectory, addressing subsequent elements individually to predict the difference in force and torque between the start and the end of the given element. As the force and torque at the end of a particular element marks the beginning of the following element, sequential calculation can be used to estimate the downhole force and torque at the end of the final element before drill bit. Reducing the length of the elements improves the accuracy of analysis and facilitates better replacement of drill path curves with straight elements. To simplify calculations, it is assumed that drill pipe lies along the bottom of the borehole for the entire HDD installation.

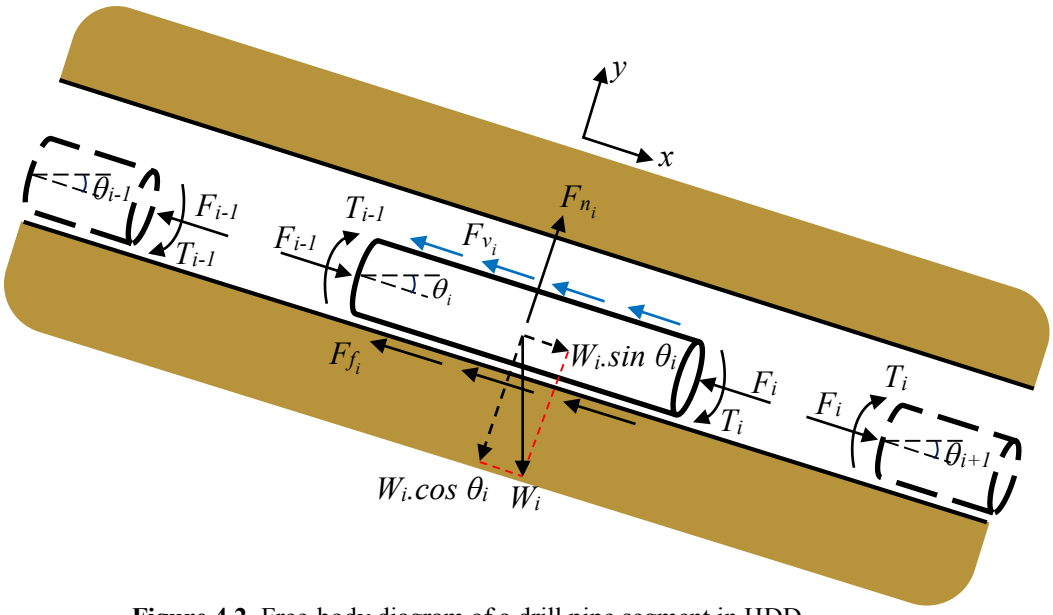

Figure 4.2. Free-body diagram of a drill pipe segment in HDD

Figure 4.2 illustrates a free-body diagram of the abovementioned forces and torques. Eqs. 4.9-4.13 present the calculation steps for the i-th element:

$$F_{n_i} = W_i.\cos\theta_i \tag{4.9}$$

$$F_{f_i} = \mu.N_i = \mu.W_i.\cos\theta_i \tag{4.10}$$

$$F_{v_i} = \pi.D_{dp}.L_i.\tau_{dp} \tag{4.11}$$

$$F_i = F_{i-1} - F_{f_i} - F_{v_i} \pm W_i.\sin\theta_i \tag{4.12}$$

$$T_i = T_{i-1} - \mu.N_i.D_{dp}/2 - \pi.D_{dp}.L_i.\tau'_{dp} \tag{4.13}$$

Where F_n is the normal force, N; F_f is the frictional force between the drill pipe and borehole, N; F_v is the viscous force on the drill pipe due to drilling fluid flow, N; W is the weight of the discretized element, N; μ is the coefficient of friction; θ is the inclination angle, degree; τ_{dp} is the viscous shear stress at the drill pipe wall due to the trip movement, Pa; τ'_{dp} is the viscous shear stress at the drill pipe wall due

to the drill pipe rotation, Pa; L is the length of the discretized element, m; and, D_{dp} is the drill pipe diameter, m.

Based on the analysis presented in Appendix A, contribution of the viscous torque in the total resisting torque was negligible and was excluded from the torque calculation for simplicity. The "+" term in Eq. 4.12 refers to elements positioned downhole, while the "–" term refers to elements positioned upslope. The viscous shear stress at the drill pipe wall is estimated based on equations describing axial flow of a Power Law fluid through two parallel plates (a slot) possessing the same annulus area (see Appendix B). Slot representation of the annulus is a commonly used assumption in HDD and oil industries for the calculation of pressure drop within the pipe and the annulus (Baroid, 1998; Bourgoyne et al., 1991). Pressure drop in the annulus and shear stress at the drill pipe wall are calculated as follows:

$$\frac{dp}{dL} = \frac{4K(8+4/n)^n \bar{v}^n}{(D_b - D_{db})^{n+1}} \tag{4.14}$$

$$\tau_{dp} = \frac{D_b - D_{dp}}{4} \frac{dp}{dL} \tag{4.15}$$

Where dp/dL is the pressure drop in the annulus, Pa/m; $\bar{v}$ is the average mud velocity inside the annulus, m/s; D_b is the bit (borehole) diameter, m; K is the Power Law consistency index, Pa-s^n; n is the Power Law flow index within the annulus.

The proposed calculation steps can be easily modeled in spreadsheet computer programs and the resistant torques and forces can be estimated at any depth in the HDD alignment. These values are then subtracted from the recorded torque and

force in real-time to determine downhole measurement, which is used to estimate downhole SE during the operation.

4.5. Application of SE in a Case Study

This section details an application of SE in an HDD installation for a river crossing in Alberta, Canada. A 311 mm (12 ¼ in) tri-cone bit and 140 mm (5 ½ in) drill pipe were used to drill a pilot hole 550 m (1800 ft) in length. Samples of drilling fluid were collected during the process and an average consistency index (K) of 5.2 Pa.s^n and a flow index (n) of 0.3 were obtained from viscometer readings during various days of operation. A fluid density of 1100 kg/m^3 (9.185 lb/gal) for the drilling mud and a constant volumetric flow rate of 1.136 m^3/min (300 gal/min) were considered in calculations. An energy reduction factor (η) of 0.25 was computed for the drill bit, and a value of 0.95 was considered for C_d (Bourgoyne et al., 1991). A coefficient of friction of 0.25 was also assumed based on the average values for the borehole friction, as recommended by Baumert et al (2005). Figure 4.3 illustrates the profile of the drill path.

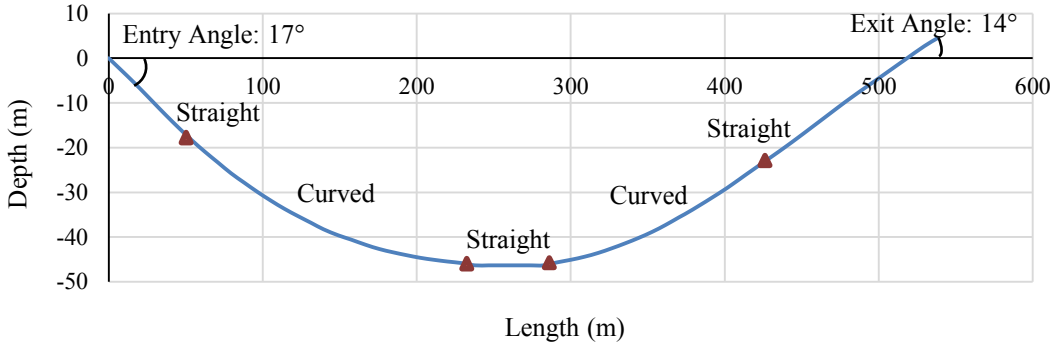

Figure 4.3. HDD drill path alignment

Figure 4.3 shows that the HDD alignment comprised three straight sections and two curved sections. The proposed methodology was used to determine resistant forces and torques in each point of the alignment. Straight sections did not need to be segmented into smaller sections and were treated as one, whole element. Conversely, each curved path was divided into twenty segments equal to the length of one drill pipe. A simple interpolation then gave the resistant loads at the middle point of the straight and curved paths. Once the resistant force and torque were calculated, the downhole loads were estimated from surface measurements. Figures 4.4 and 4.5 show surface thrust and torque measurement versus downhole predictions determined by the proposed method. At the beginning of the drilling process, effective force and torque available for the drill bit is identical to the input loads provided by the rig. As the drill bit advances, the difference between surface

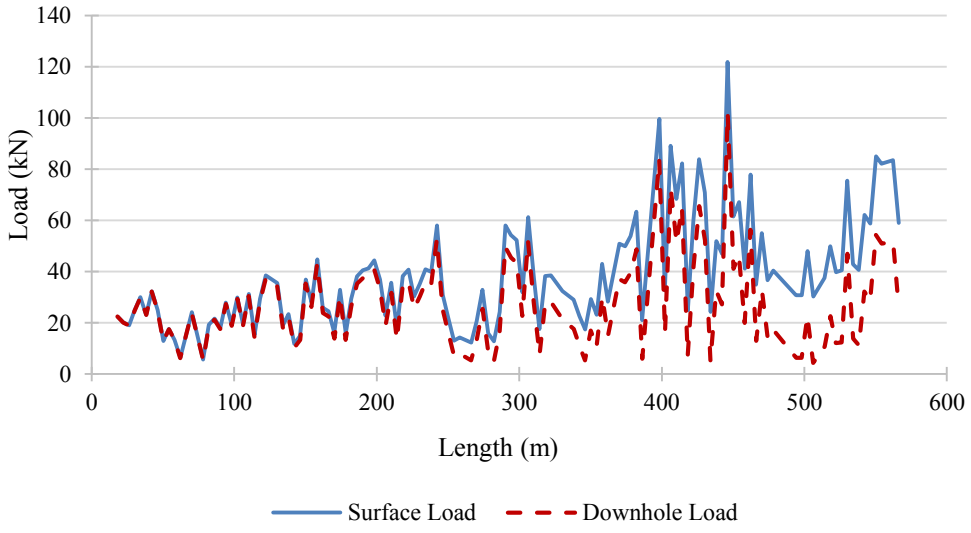

Figure 4.4. Surface load versus predicted downhole load

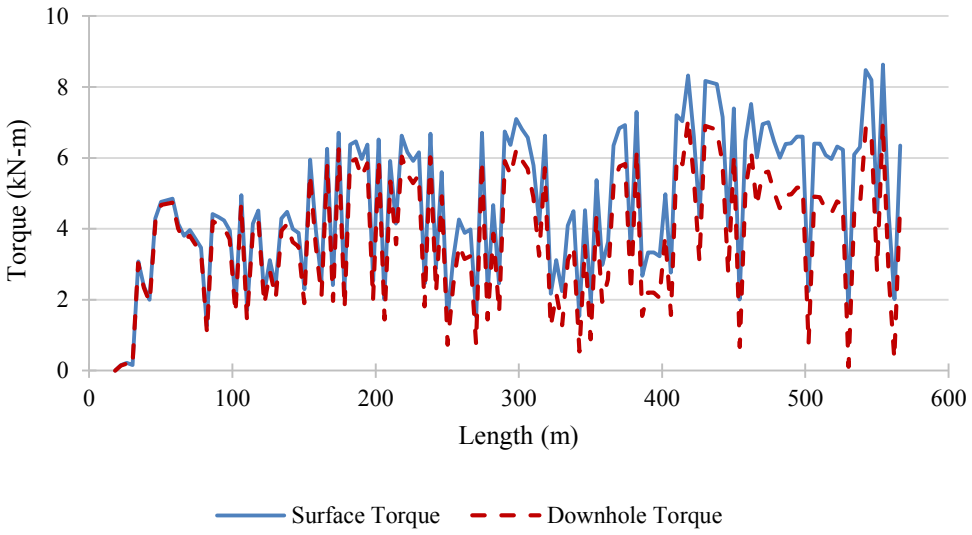

Figure 4.5. Surface torque versus predicted downhole torque

and downhole measurements increases due to additional energy loss from the friction experienced by the drill pipes within the borehole. These losses amounted to 32 kN in thrust and 1.7 kN-m in torque at the end of the drilling.

Figure 4.6 shows the calculated downhole SE as well as its thrust, rotary, and hydraulic components to compare the significance of each term. The thrust component's contribution to specific energy is very small (Figure 4.6), and the majority of the drilling work is completed by the rotary and hydraulic energies. However, the insignificance of the thrust component corresponds to the normal drilling condition of this case. In other cases where the drill bit may stick, the friction forces will build up and the thrust energy will increase considerably.

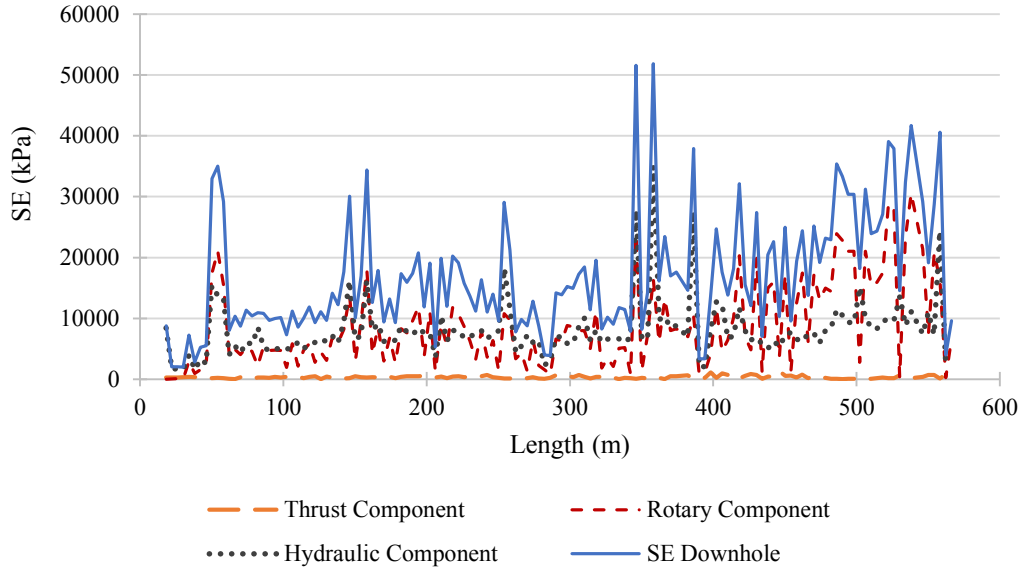

Figure 4.6. Downhole specific energy and contribution of thrust, rotary, and hydraulic components

Figure 4.7 shows the surface and downhole SE and indicates that the difference between the two accumulated to 11000 kPa in the final sections of the profile. The longer the drill path is, the more significant the difference becomes. Therefore, an inevitable growth in surface SE is observed as the drill bit advances due to the greater amount of energy loss. Hence, the criterion to notify the operator of any inefficiency during operations is the downhole SE as it indicates the actual energy spent by the bit. The variation between surface and downhole SE is mainly caused by the difference between downhole and surface torque and, to a minor extent, by the thrust component. The hydraulic energy calculation is almost the same for both surface and downhole SE.

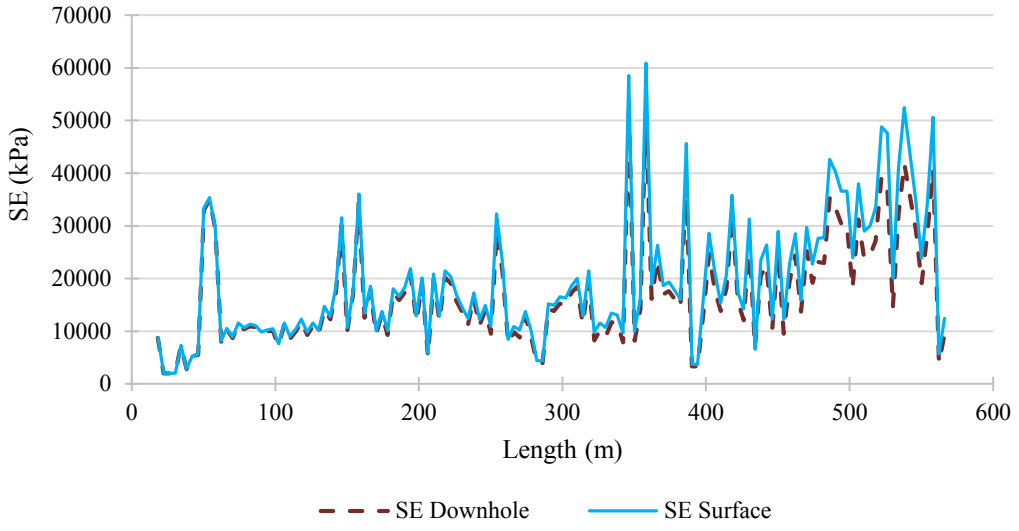

Figure 4.7. Comparison of surface versus downhole SE

To evaluate the efficiency of drilling, SE surveillance should be coupled with the ROP. Figure 4.8 shows the ROP of the drilled pilot hole. Figure 4.7 and 4.8 enable the operators to identify the locations of possible inefficiencies or changes in formation. These data together with geotechnical and lithology information give the rig site operators a powerful tool to identify underground risks and uncertainties. For instance, drilling began with a high ROP that corresponded to a low SE. It was then followed by a drop in ROP for the next 20 m along the drill path, resulting in a jump in SE. This increase was likely the result of the drill bit hitting a harder formation or an inefficiency condition lowering the drill rate. HDD personnel can do similar analyses to explain drilling problems they face during a project. SE surveillance is an effective educational tool that gives HDD operators valuable information regarding underground conditions.

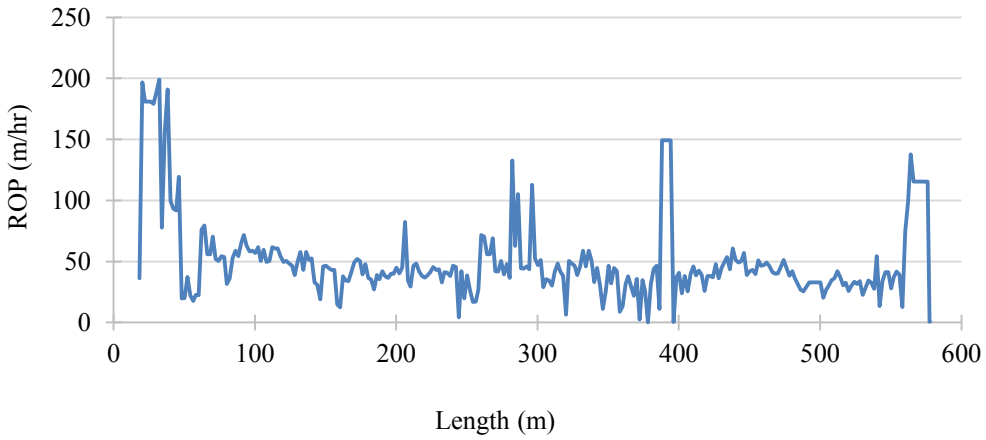

Figure 4.8. Rate of penetration for the case study

4.6. Conclusions

The concept of specific energy was introduced in this chapter as an efficiency indicator during HDD operations. A method has been presented to calculate the energy losses and predict downhole thrust and torque from surface measurements. A case study was used to demonstrate the SE calculated based on surface and downhole conditions. The results revealed that the drill pipe friction within the borehole and the viscous drilling fluid reduced the amount of effective load and torque available for the drill bit as excavation advanced. It was also concluded that the rotary and hydraulic energies comprised a greater proportion of the energy expended by the bit in comparison to the thrust component. Locations on the drill path with high SE are indicators of potential inefficiency condition that can be addressed and eliminated by the rig personnel. Real-time SE analysis can be used as a tool with the potential to significantly improve the HDD process.

5. Chapter 5: Summary and Conclusions

5.1. Summary

Horizontal Directional Drilling (HDD) is one of the most versatile technology amongst trenchless methods to meet the needs for development of the utility infrastructure. The rapid growth in use of HDD has not accompanied the same level of development in engineering design models and efficiency measurement techniques. Lack of accurate methods to calculate viscous drag exerted on the drill pipe and product pipe led to further analysis in this thesis and the exact equations to calculate fluidic drag were developed to check the reliability of the common design procedures such as ASTM 1962 and PRCI. This attempt was made to improve the design phase of HDD operations when estimation of the fluidic drag in the pullback load is necessary and accuracy of calculations will lead to major cost savings.

Furthermore, the concept of Specific Energy (SE) in drilling was selected to be implemented in HDD for the first time to improve drilling operations. Calculation of the real amount of energy used by the drill bit required to record downhole drilling data. Having reliable downhole data without the installation of expensive downhole measuring tools necessitated the development of a model to compute the loads and torques exerted to the drill bit. Using the results of previous analysis on viscous drag enabled the development of a mechanical model for prediction of downhole data. Downhole calculations were compared with the surface

measurement in a real case study and SE was calculated for surface and downhole conditions.

5.2. Conclusions

In this research, exact annular flow equations were used to calculate the viscous drag exerted to the drill pipe and the product pipe during HDD and analysis revealed that:

- The fluidic drag predicted by the proposed method was about 8% of the maximum rig load.
- PRCI overestimated the fluidic drag excessively, while ASTM F1962 resulted in a closer prediction to the maximum drag calculated by the proposed model.
- Results of a sensitivity analysis on the viscous drag revealed that the ratio of the pipe radius to borehole radius has a noticeable impact on the amount of the drag and increasing the ratio means tighter annular space and larger load is needed to overcome fluidic drag.
- The overall thickness of the drilling fluid represented by the Power Law consistency coefficient ranked as the second influential parameter on the viscous drag and higher values of fluidic drag are expected in a more viscous and thicker drilling fluid.
- On the contrary, the effect of the pipe speed (pullback speed) is negligible on fluidic drag.

A proposed analytical model was used to calculate the energy losses by the drill pipe and predict downhole thrust and torque from surface measurements. A real case study was considered and SE was computed for surface and downhole conditions and it was observed that:

- The drill pipe interaction with the borehole and the viscous drilling fluid reduces the amount of effective energy available for the drill bit as longer lengths of crossing is being excavated.
- Most of the drilling process is done by the rotary and hydraulic energies and thrust component of SE is almost negligible.
- SE can be calculated real-time and be used to analyze the efficiency of the drilling in HDD and identify the problems that may occur during the operation.

5.3. Future Research

This study provided the methodology to use the concept of SE in HDD. Complete implementation of SE in HDD will be accomplished by further energy analysis during real projects and explaining the drilling problems from the energy point of view. Therefore, it is recommended to use SE in further operations to identify how much cost and time saving will be achieved. Moreover, field experiments can be conducted to evaluate the significance of mechanical and hydraulic parameters during pilot hole drilling. Simple try and error approach by the driller can result in finding the optimum drilling parameters to get the maximum

ROP. Then, efficient and inefficient regions of drilling can be obtained similar to the traditional WOB vs ROP curve in oil field. It is also recommended to use the energy concept in design of the drill bits in order to improve their performance.

6. References

Abraham, D., and Gokhale, S. (2002). "Development of a decision support system for selection of trenchless technologies to minimize impact of utility construction on roadways." *Joint Transportation Research Program*, 60.

Ali, S., Zayed, T., and Hegab, M. (2007). "Modeling the effect of subjective factors on productivity of trenchless technology application to buried infrastructure systems." *Journal of Construction Engineering and Management*, 133(10), 743-748.

Allouche, E. N., Ariaratnam, S. T., and Lueke, J. S. (2000). "Horizontal directional drilling: profile of an emerging industry." *Journal of Construction Engineering and Management*, 126(1), 68-76.

Allouche, E. N., Ariaratnam, S. T., and MacLeod, C. W. (2003). "Software for planning and cost control in directional drilling projects." *Journal of construction engineering and management*, 129(4), 446-453.

American Petroleum Institute (API). (1995). "Recommended practice on the rheology and hydraulics of oil-well drilling fluids API RP 13D." Washington, D.C, USA.

American Society for Testing and Materials (ASTM). (1999). "Standard guide for use of maxi-horizontal directional drilling for placement of polyethylene pipe or conduit under obstacles, including rivers F 1962-99." West Conshohocken, Pa.

American Society for Testing and Materials (ASTM). (2011). "Standard guide for use of maxi-horizontal directional drilling for placement of polyethylene pipe or conduit under obstacles, including rivers F 1962-11." West Conshohocken, Pa.

Ariaratnam, S. T., Lueke, J. S., and Allouche, E. N. (1999). "Utilization of trenchless construction methods by Canadian municipalities." *Journal of construction engineering and management*, 125(2), 76-86.

Ariaratnam, S. T., and Allouche, E. N. (2000). "Suggested practices for installations using horizontal directional drilling." *Practice Periodical on Structural Design and Construction*, ASCE, 5(4), 142-149.

Ariaratnam, S. T., Harbin, B. C., and Stauber, R. L. (2007). "Modeling of annular fluid pressures in horizontal boring." *Tunnelling and underground space technology*, 22(5), 610-619.

Armenta, M. (2008). "Identifying inefficient drilling conditions using drilling-specific energy." *Proc., SPE Annual Technical Conference and Exhibition*, Denver, Colorado.

Atalah, A., Kariuki, J., and Najafi, M. (2009). "Cost Comparison between horizontal directional drilling and open-cut construction methods in Nairobi, Kenya." *Journal of construction engineering and management,* 361(41073), 144.

Baroid Fluids Handbook. (1998). Baroid Drilling Fluids, Inc. Houston, TX.

Baumert, M. E., and Allouche, E. N. (2002). "Methods for estimating pipe pullback loads for horizontal directional drilling (HDD) crossings." *Journal of infrastructure systems*, 8(1), 12-19.

Baumert, M. E., Allouche, E. N., and Moore, I. D. (2005). "Drilling fluid considerations in design of engineered horizontal directional drilling installations." *International Journal of Geomechanics*, *5*(4), 339-349.

Bevilacqua, M., Ciarapica, F. E., and Marchetti, B. (2013). "Acquisition, processing and evaluation of down hole data for monitoring efficiency of drilling processes." *Journal of Petroleum Science Research*, 2(2), 49-56.

Bonet, L., Cunha, J. C. S. and Prado, M. G. (1995). "Drilling optimization: a new approach to optimize drilling parameters and improve drilling efficiency." Drilling Technology, ASME.

Bourgoyne Jr, A. T., and Young Jr, F. S. (1974). "A multiple regression approach to optimal drilling and abnormal pressure detection." *Society of Petroleum Engineers Journal*, 14(4), 371-384.

Bourgoyne, A. T., Chenevert, M. E., Millheim, K. K., and Young, F. S. (1991). "Applied drilling engineering." SPE Textbook Series, Vol. 2, Richardson, TX.

Caicedo, H. U., Calhoun, W. M., and Ewy, R. T. (2005). "Unique ROP predictor using bit-specific coefficient of sliding friction and mechanical efficiency as a function of confined compressive strength impacts drilling

performance." *Proc., SPE/IADC Drilling Conference and Exibition*, Amsterdam, The Netherlands.

Chehab, A.G., Moore, I.D. (2008). "Polymer pipes in trenchless applications: HDPE pipe response during pulled in place installation." *Proc., Geoamericas*: *the First Pan American Geosynthetics Conference and Exhibition*, Cancun, Mexico.

Chhabra, R. P., and Richardson, J. F. (1999). "Non-Newtonian flow in the process industries." Oxford, Boston, MA, Butterworth-Heinemann.

Deneen, M. (2013). "World oil and gas pipe demand to reach 51.8 million metric tons in 2017." *Pipeline and Gas Journal*, 240(12). Retrieved from http:// http://www.pipelineandgasjournal.com/world-oil-and-gas-pipe-demand-reach-518-million-metric-tons-2017?page=show.

Drillpath™, (1996). "Theory and user's manual." Infrasoft L. L. C., Houston, Texas, USA.

Driscopipe. (1993). "Technical expertise application of driscopipe in directional-drilling and river-crossings." Tech. Note No. 41.

Dupriest, F. E., and Koederitz, W. L. (2005). "Maximizing drill rates with real-time surveillance of mechanical specific energy." *Proc., SPE/IADC Drilling Conference and Exibition*, Amsterdam, The Netherlands.

Dupriest, F. E., Witt, J. W., and Remmert, S. M. (2005). "Maximizing ROP with real-time analysis of digital data and MSE." *Proc., International Petroleum Technology Conference*, Doha, Qatar.

Dupriest, F. E. (2006). "Comprehensive drill rate management process to maximize ROP." *Proc., SPE/IADC Drilling Conference and Exibition*, San Antonio, Texas, USA

Duyvestyn, G. (2009). "Comparison of predicted and observed HDD installation loads for various calculation methods." *Proc., International No-Dig Show*, Toronto, Ontario.

Fredrickson, A., and Bird, R. B. (1958). "Non-Newtonian flow in annuli." *Industrial and Engineering Chemistry*, 50(3), 347-352.

Guerrero, C. A., and Kull, B. J. (2007). "Deployment of an SeROP Predictor Tool for Real-Time Bit Optimization." *Proc., SPE/IADC Drilling Conference and Exibition*, Amsterdam, The Netherlands.

Haciislamoglu, M., and Langlinais, J. (1990). "Non-Newtonian flow in eccentric annuli." *Journal of energy resources technology*, 112(3), 163-169.

Haciislamoglu, M., and Langlinais, J. (1991). "Effect of Pipe Eccentricity on Surge Pressures." *Journal of Energy Resources Technology*, 113(3), 157-160

Hanks, R. W., and Larsen, K. M. (1979). "The flow of Power Law non-Newtonian fluids in concentric annuli." *Industrial and Engineering Chemistry Fundamentals*, 18(1), 33-35.

Huey, D. P., Hair, J. D., and McLeod, K. B. (1996). "Installation loading and stress analysis involved with pipelines installed in horizontal directional drilling." *Proc., International No-Dig Show*, New Orleans, LA, USA.

Koederitz, W.L and Weis, J (2005). "A real-time implementation of MSE." *Proc., AADE National Technical Conference and Exhibition*, Houston, Texas.

Mahmoud, M. A. (2009). "Productivity analysis of horizontal directional drilling." M.S. thesis, Concordia University, Montreal, Quebec, Canada.

Mitchell R.F, Miska S., and Aadnoy B.S. (2011). "Fundamentals of drilling engineering." Richardson, TX: Society of Petroleum Engineers.

Mohan, K., Adil, F., and Samuel, R. (2009). "Tracking drilling efficiency using hydro-mechanical specific energy." *Proc., SPE/IADC Drilling Conference and Exibition*, Amsterdam, The Netherlands.

Najafi, M. (2005). "Trenchless technology: pipeline and utility design, construction, and renewal." McGraw-Hill, New York.

Najafi, M. (2010). "Trenchless technology piping: installation and inspection." McGraw-Hill, New York.

Najafi, M. (2014). "Trenchless technology: pipeline and utility design, construction, and renewal." McGraw-Hill, New York.

NEN (1992). "Requirements for steel pipeline transportation systems." NEN 3650 (unofficial translation), Government/Industry Standards Committee 343 20, The Netherlands.

Origho, B. E. (2012). "Incorporating an effective torque from a torque and drag model into the concept of mechanical specific energy." M.S. thesis, Montana Tech of The University of Montana, U.S.

Osbak, M. (2011). "Geotechnical investigations for tunneling using horizontal directional drilling." *Proc., of Rapid Excavation and Tunneling Conference (RETC)*, San Francisco, CA, USA.

Osbak, M. (2011). "Theory and application of annular pressure management." *Proc., International f the No-Dig Conference*, Washington, D.C., USA.

Pessier, R. C., and Fear, M. J. (1992). "Quantifying common drilling problems with mechanical specific energy and a bit-specific coefficient of sliding friction." *Proc., SPE/IADC Drilling Conference and Exibition*, Washington, D.C, USA.

Pessier, R. C., Wallace, S. N., and Oueslati, H. (2012). "Drilling performance is a function of power at the bit and drilling efficiency." *Proc., SPE/IADC Drilling Conference and Exibition*, San Diego, CA, USA.

Plastics Pipe Institute®, Handbook of Polyethylene Pipe, (2009). Chapter 12, Horizontal Directional Drilling.

Polak, M. A., and Lasheen, A. (2001). "Mechanical modelling for pipes in horizontal directional drilling." *Tunnelling and underground space technology*, 16(1), 47-55.

Provost Jr, C. E. (1987). "A real-time normalized rate of penetration aids in lithology and pore pressure prediction." *Proc., SPE/IADC Drilling Conference and Exibition*, New Orleans, LA, USA.

Puckett, S. (2003). "Analysis of theoretical versus actual HDD pulling loads." *Proc., ASCE Pipeline Conference*, Baltimore, Maryland.

Rabia, H. (1985). "Specific energy as a criterion for bit selection." *Journal of petroleum technology*, 37(8), 1225-1229.

Reed, R. L. (1972). "A monte carlo approach to optimal drilling." *Society of Petroleum Engineers Journal*, 12(5), 423-438.

Remmert, S. M., Witt, J. W., and Dupriest, F. E. (2007). "Implementation of ROP management process in Qatar north field." *Proc., SPE/IADC Drilling Conference and Exibition*, Amsterdam, The Netherlands.

Sarireh, M. (2011). "Development of a model for productivity of horizontal directional drilling (HDD)." Ph.D. thesis, The University of Texas at Arlington, Texas, U.S.

Sarireh, M., Najafi, M., Slavin, L. (2012). "Usage and applications of horizontal directional drilling." *Proc., of International Conference of Pipelines and Trenchless Technology*, Wuhan, China.

Teale, R. (1965). "The concept of specific energy in rock drilling." *International Journal of Rock Mechanics and Mining Sciences and Geomechanics*, 2(1), 57-73.

Trenchless Technology. (2011). Horizontal Directional Drilling Guide. Trenchless Technology Supplements. Retrieved from www.trenchlessonline.com.

Warren, T. M. (1987). "Penetration rate performance of roller cone bits." *Society of Petroleum Engineers Journals*, 2(1), 9-18.

Waughman, R. J., Kenner, J. V., and Moore, R. A. (2002). "Real-time specific energy monitoring reveals drilling inefficiency and enhances the

understanding of when to pull worn PDC bits." *Proc., SPE/IADC Drilling Conference and Exibition*, Dallas, Texas.

Willoughby, D. (2005). "Horizontal directional drilling: utility and pipeline applications." McGraw-Hill, New York.

Wojtanowicz, A. K., and Kuru, E. (1993). "Minimum-cost well drilling strategy using dynamic programming." *Journal of energy resources technology*, 115(4), 239-246.

Zayed, T., Amer, M. I., Dubey, B., and Gupta, M. (2007). "Deterministic productivity model for horizontal directional drilling." *Proc., Twelfth international colloquium on structural and geotechnical engineering*, Cairo, Egypt.

Appendix A: Calculation of Viscous Torque on Drill Pipe

Viscous torque is caused by the hydraulic friction due to the drill pipe rotation inside the borehole. Since there is no direct analytical solution to calculate viscous torque, analysis for a rotational viscometer given in Applied Drilling Engineering is used to show the effect of this factor on downhole torque predictions (Wellplan, 1998).

Shear rate at the wall of the drill pipe ($\dot{\gamma}_{dp}$, s^{-1}) due to the drill pipe rotation is given as:

$$\dot{\gamma}_{dp} = \frac{4\pi.RPM/60}{D_{dp}^{\ 2}(1/D_{dp}^{\ 2} - 1/D_h^{\ 2})} \tag{A.1}$$

Where, D_{dp} and D_h are the drill pipe and the borehole diameter, respectively, m; and RPM is the drill pipe rotational speed, rev/min. Given the shear rate, the shear stress is calculated from the rheological properties of the fluid. In case of Power Law, the shear rate at the drill pipe wall (τ_{dp}, Pa) is:

$$\tau_{dp} = K\dot{\gamma}^n \tag{A.2}$$

Where K is the Power Law consistency index, $Pa.s^n$. Torque on the drill pipe is then calculated from the product of shear stress, the surface area of the drill pipe, and the torsional radius:

$$T_v = 2\pi.L(D_{dp}/2)^2\tau_{dp} \tag{A.3}$$

Where, T_v is the viscous torque on the drill pipe, N.m, and L is the length of the drill pipe, m.

The torque given to the drill pipe by the drill rig is resisted by the frictional torque and the viscous torque within the borehole and downhole torque is obtained by subtracting them from the surface torque. Viscous torque was computed for the case study in chapter 4, and it was graphed versus the frictional torque along the drill path in Figure A.1. The figure shows that resistant torques increased as longer length of drill pipe situated in the borehole and the contribution of the viscous torque in calculation of the downhole torque is negligible in comparison with the frictional torque. Therefore, viscous torque calculation was skipped to simplify the proposed model in chapter 4.

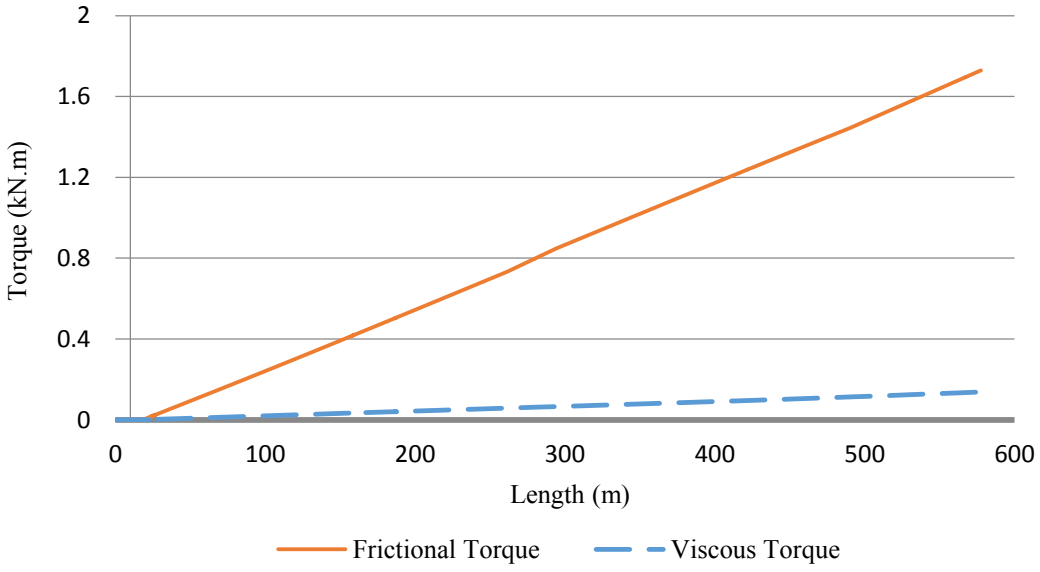

Figure A.1. Frictional torque versus viscous torque along the drill path.

Appendix B: Calculation of Viscous Force on Drill Pipe

The exact flow equations for a concentric annulus were presented in chapter 3. However, using those equations to calculate the viscous force on the drill pipe is complicated and far from field application. Other available methods to compute the viscous drag are limited to PRCI procedures, which is given to calculate the drag during steel pipe installation, and the flow equations based on the slot representation of the annulus.

Equations describing liquid flow in the annulus can be approximated assuming that the fluid flows through two parallel plates with the same annular area (Skelland, 1967; Craft et al., 1962; Bird et al., 1960; Savins, 1958; Azar, 1979). These researchers show that a rectangular slot can model the axial laminar flow in a concentric annulus with a good accuracy. The slot representation of annular flow has higher degree of accuracy when the ratio of the pipe's radius to the bore's radius is at least 0.3. As proved in chapter 3, the influence of the drill pipe speed is negligible. Therefore, the common equations in drilling engineering derived by the concept of flow through a slot can be used. Consequently, pressure drop in the annulus and shear stress at the drill pipe wall are calculated as follow:

$$\frac{dp}{dL} = \frac{4K(8+4/n)^n \bar{v}^n}{(D_b - D_{db})^{n+1}} \tag{B.1}$$

$$\tau_{dp} = \frac{D_b - D_{dp}}{4} \frac{dp}{dL} \tag{B.2}$$

Where *dp/dL* is the pressure drop in the annulus, Pa/m; $\bar{v}$ is the average mud velocity inside the annulus, m/s; D_b and D_{dp} are the bit (borehole) diameter and the drill pipe diameter, respectively, m; *K* is the Power Law consistency index, Pa-s^n; and *n* is the Power Law flow index within the annulus.

Figure B.1 shows the viscous force on the drill pipe computed for the case study of the chapter 4 based on the exact solution presented in chapter 3, PRCI method, and Eqs. B.1 and B.2. It can be seen that the equations by the slot representation of the annulus predicted viscous drag close to the exact solution, while PRCI gives higher forces. Hence, Eqs. B.1 and B.2 were used to calculate downhole thrust by the proposed model in the chapter 4 as an easier alternative for the exact annular flow equations.

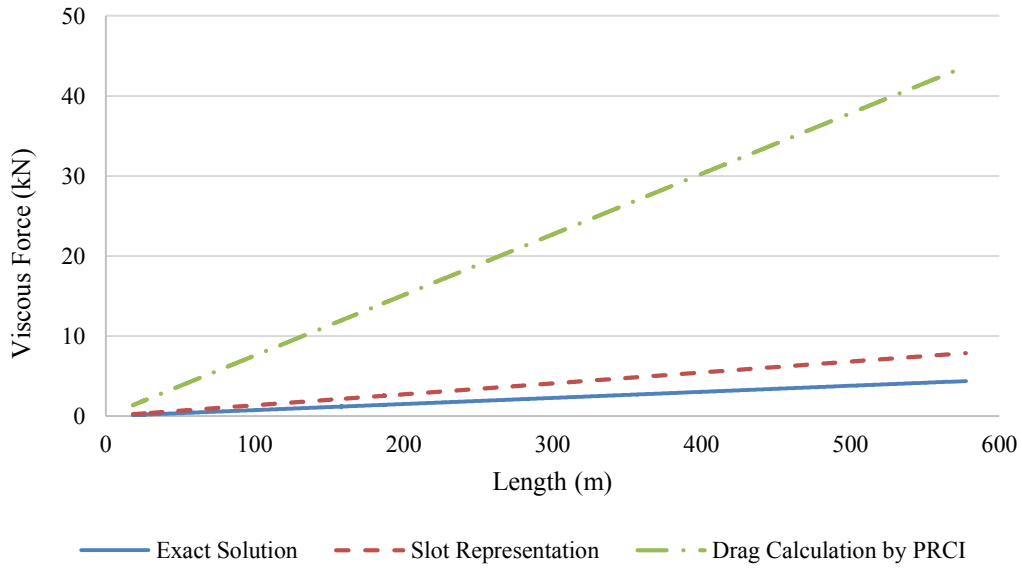

Figure B.1. Viscous force on the drill pipe calculated by different methods.

Refrences of Appendices

Azar, J. J. (1979). "Drilling in petroleum engineering." Preprint, Petroleum Publishing Co., Tulsa 265-268.

Bird, R. B., Stewart, W. E., and Lightfoot, E. N. (1960). "Transport Phenomena." John Wiley and Sons Inc., New York City.

Craft, B. C., Holden, W. R., and Graves, E. E. Jr. (1962). "Well design: drilling and production." Prentice-Hall Inc., Englewood Cliffs, NJ 55-79.

Savins, J .G. (1958). "Generalized Newtonian (pseudoplastic) flow in stationary pipes and annuli." *AIME* 213, 325-332.

Skelland, A. H. P. (1967). "Non-Newtonian flow and heat transfer." John Wiley and Sons Inc., New York City.

Wellplan. (2004). "User manual and program guide." Version R2003.11.0.1, Landmark Graphics Corporation.